ACTIVATED CARBON, BIOCHAR, AND LIGNOCELLULOSIC DERIVATIVE MATERIALS FOR REMOVING ANTIBIOTICS FROM WATER: AN OVERVIEW

CAMILA NEGRETE-VERGARA[1], GABRIEL SALFATE[2], ESTEFANÍA OYARCE[2], KARINA ROA[2], ANDRÉS BOULETT[2], JULIO SÁNCHEZ[3], AND BERNABÉ L. RIVAS[4]*

[1] *Department of Chemistry, Biochemistry and Pharmaceutical Sciences, University of Bern.Bern 3012, Switzerland.*
[2] *Universidad de Santiago de Chile (USACH), Santiago, Chile.*
[3] *Departamento de Química Orgánica, Facultad de Química y de Farmacia, Pontificia Universidad Católica de Chile, Santiago, Chile.*
[4] *Universidad San Sebastián, Concepción, Chile.*

ABSTRACT

Antibiotics have improved the quality of life of human society due to their applications in medicine and food production. Nevertheless, antibiotics are also considered emerging pollutants because they have been found in the environment, water sources, and tap water. Their chemical stability and the excessive usage of these substances are the main causes of their presence in the environment. Antibiotics can be removed from water using adsorbent materials, in which activated charcoal has been extensively used for removing organic pollutants. Concerns about the environmental impact of producing activated charcoal are placing the interest in new eco-friendly materials for organic pollutant removal from water such as biochar and lignocellulosic materials. Those materials have desirable properties that allow them to remediate water in the presence of antibiotics.

In this study, the use of activated carbon, biochar, and lignocellulosic materials for removing antibiotics from water is reviewed. Here we discuss the advantages and limitations of each material for the aforementioned purpose, comparing their efficiency in the removal of common antibiotics used in healthcare and agroindustry, and considering new approaches and alternatives to the technologies used for antibiotic removal from water.

Keywords: Lignocellulose, activated carbon biochar, adsorption, antibiotic, pollution.

INTRODUCTION

An antibiotic is a substance that in low amounts (usually expressed as a minimum inhibitory concentration in μg mL^{-1}) is toxic to microorganisms [1]. Since the discovery of penicillin in 1928, antibiotics have shaped the contemporary world, improving the quality of life of human beings. Healthcare systems and food production depend on the usage of antibiotics [1–4]. However, the extensive usage of these substances, especially in the agroindustry is causing a crisis involving aspects related to antibiotic resistance and pollution [5]. Antibiotics have been detected in water sources and water treatment plants, being considered "emerging pollutants" because of their chemical and biochemical properties that make them effective against pathogenic microorganisms, such as chemical stability and the ability to be eliminated from the body as unchanged molecules, allow their presence and accumulation in soils and waters, disrupting ecosystems and adding sources for the development of antibiotic resistance [6–9].

Antibiotics have been found in water sources, wastewater treatment plants, and tap water in different amounts, which mainly depend on their chemical stability. For example, fluoroquinolones and macrolides have been found in municipal wastewater in China with mean concentrations of 4916 ng L^{-1} and 365 ng L^{-1} have been documented [10]. Wastewater effluents from industrial areas in India have an alarmingly high amount of fluoroquinolones, up to 31 mg L^{-1} [11]. Fluoroquinolones have been found in tap water in China [10]. Macrolides, fluoroquinolones, tetracyclines (TC), and sulfonamides (SNs) have been detected in rivers across various countries including the United States, Spain, Italy, France, South Korea, Taiwan, and China. Concentrations of these substances ranged from 3.00 ng L^{-1} to 17.0 μg L^{-1}. In African rivers, SNs have been detected at concentrations reaching up to 53.0 μg L^{-1} [10,11]. Groundwater analyses have found fluoroquinolones and sulphonamides, ranging from 323 ng L^{-1} to 3460 ng L^{-1} [24]. In seawater and sediments, macrolides, TC, and SNs have been found, ranging from 0.100 ng L^{-1} to 16.0 ng L^{-1} in seawater, and 1.00 μg kg^{-1} to 63.0 μg kg^{-1} in sediments [10].

Different techniques have been proposed to remove antibiotic pollutants from water [12,13]. Nevertheless, using adsorption to remove pollutants is still the most practical approach due to their advantages: high efficiency, high capacity for capturing pollutants, energetic efficiency, facility to implement, and scale for industrial needs [14–16]. Adsorbents are classified as inorganic/mineral adsorbents, carbon-based adsorbents, which include activated carbon (AC), biochar (BC), and other adsorbents. These include synthetic and natural polymers and composites [16]. AC has been used extensively as an adsorbent for the remediation of different organic species from water. AC is denoted as an effective and preferred material for the adsorption of different organic pollutants, including antibiotics. However, AC is commonly generated from non-renewable carbon sources and thermally activated in the presence of an oxidizing agent (commonly steam). This process is called physical activation and implies a high economic and energetic cost [17]. Chemical activation carries a negative environmental impact since it requires the use of chemical agents, such as phosphoric acid, zinc chloride, and sulfuric acid [18,19]. In this context, the elaboration process of AC on a large scale is considered one of the drawbacks to producing ecological and low-cost adsorbent materials. A potential alternative is the preparation of AC through carbonized biomass or biowaste materials which is commonly known as BC when is carbonized in anoxia conditions (absence of oxygen) and physical or chemical activation is avoided [18,19]. In recent years, materials based on lignocellulosic biomass, namely cellulose and lignin, have also been employed as effective adsorbents of antibiotics demonstrating good adsorption capacity [20-22].

Due to the large interest and urgent need to eliminate antibiotics from water, several research groups have focused on this relatively young field, illustrating its growth, and reflecting the perceived potential of different adsorbents from biomass or biowastes. In this regard, several review articles highlighting the developments in this field have appeared in rapid succession. These reviews have emphasized various aspects. For instance, Ahmed et al. [20] presented in 2015 a review of the progress and challenges for the adsorptive removal of antibiotics in water and wastewater, offering critical analysis and a summary of the research done until that year by using AC, BC, carbon nanotubes, mineral clays, resins, and graphite as adsorbents. BCs were positively evaluated in that work, emphasizing the potential as low-cost material and efficient adsorbent. Furthermore, some hints regarding the antibiotic adsorption mechanism were exposed, which involves π–π EDA interactions, electrostatic interactions, hydrophobic interaction, hydrogen bonds, and pore filling. Some years later, Malakootian et al. [21] presented a systematic review with a focus on the potential of nanoparticles for the removal of diverse antibiotics organized by their classification, highlighting that nanoparticles offer a good solution for antibiotics uptake. However, some disadvantages such as cost, synthesis, toxicity on humans and other organisms could hinder their application. In a similar vein, but putting the focus on the adsorbent material, Eniola et al. [19] reviewed the removal of antibiotics over natural and modified adsorbents. They found that the best efficacy for antibiotic uptake is performed by hybrid materials, pointing out the importance of material modification, for improving the morphology and stability of the adsorbent. Later on, attention was turned to the development of adsorbents based on BCs for antibiotic removal. In this regard, Krasucka et al. [18] reviewed, to that date, the latest advances in the field, involving BC-based materials. The focus was on emerging biochar modification and biochar composite approaches, and the interaction of antibiotics/adsorbents that could generate tailored materials with enhanced adsorption performance. Over the past

*Corresponding author email: julio.sanchez@uc.cl

year, the scientific community and public health organizations have become increasingly aware of high levels of antibiotics in aquatic ecosystems and other water sources. As mentioned before, these concentrations pose a potential threat to both human and ecological health. For this reason, different authors have critically reviewed the remediation strategies for antibiotics in water sources. For example, Alegbeleye et al. [22] critically assessed twelve different methods for the removal of antibiotics. The authors provided a detailed analysis of various techniques including chlorination, ozonation, UV irradiation, Fenton process, photocatalysis, electrochemical oxidation, plasma treatment, adsorption by BC, AC, and nanomaterials, as well as anaerobic digestion. Overall, the treatments mentioned can be regarded as efficient, eliminating, or significantly reducing the level of antibiotics. On a similar note, Mangla et al [23] focused on the adsorptive removal of antibiotics, critically reviewing "so-called" unconventional adsorbents including BC, biopolymers, carbon nanotubes, clays, metal-organic frameworks, microalgae, and some miscellaneous adsorbents. Among these, biopolymer-based adsorbents have been pointed out as an effective material for antibiotic adsorption, as well as having the least ecological impact, compared to non-biodegradable adsorbents.

The present overview is focused on an updated and exhaustive revision of the materials and biomaterials that are most used as antibiotic adsorbents, highlighting AC, BC, and lignocellulosic materials. Compared to other remediation techniques, these adsorbents have the potential to be more environmentally friendly.

CHEMISTRY OF ANTIBIOTICS

Antibiotics can be classified according to their chemical structure and spectrum of activity [1]. **Table S1** shows relevant information about the classification of common chemical structures presented in antibiotics and their mechanism of action.

Penicillin and cephalosporin are common antibiotics referred to as β-lactam antibiotics, which share a four-membered heterocyclic ring in their structure. The stability of penicillins in aqueous media differs among them and they are usually unstable in acid and alkaline media. Some penicillins, like penicillin G (PNG) benzathine, are water-insoluble. However, all penicillins are eliminated from the body mostly unchanged through urine. Most penicillins are sensitive to β-lactamases enzymes produced by bacteria, which is the source of penicillin-resistant-pathogens. Considering their chemical structure, cephalosporins, and penicillins have in common the β-lactam ring, but cephalosporins present greater chemical stability compared to penicillins because they have a six-membered heterocyclic ring attached to the β-lactam ring decreasing the structural tension present in the four-membered heterocyclic ring, making them more chemical and biochemically resistant than penicillins. Cephalosporins are polar compounds with different solubility in water and are more stable than penicillins in acidic media [24].

In contrast, aminoglycoside antibiotics are a class of low-molecular-weight compounds characterized by amino-substituted saccharide derivatives. These antibiotics are composed of inositol-saturated rings consisting of six-membered and five or six-carbon sugars, connected by glycosidic bonds. The presence of amino groups attached to the rings, together with the hydroxyl groups present in the saccharides, makes them water-soluble and alkaline compounds [25].

Macrolide antibiotics are a large six-to-fourteen carbon lactone ring attached to at least one sugar bonded by glycosidic bonds. The lactone ring could be substituted by alkyl, ketone, aldehyde, and amino groups. They are usually unstable in acidic media [26,27].

Fluoroquinolone antibiotics are bicyclic compounds derived from quinolone, with a fluorine atom bonded to the aromatic ring. They are amphoteric due to the presence of both amino- and carboxylic-containing groups. Fluoroquinolones have low water solubility between pH 6.00 – 8.00 and are prone to precipitation in acidic media. They are mostly excreted as uncharged molecules through urine [28,29].

Tetracycline (TC) antibiotics are linearly arranged four-ring molecules that possess keto-enol functional groups that allow them to coordinate metal cations. TC antibiotics are water- soluble and, due to the presence of reactive chemical groups in their structure, they are sensitive to pH conditions, being more stable in acid, but not in alkaline medium [30,31].

Nitrofuran antibiotics are five-membered heterocyclic compounds with an azomethine, and nitro group attached. They are mainly used in human and veterinary medicine for the treatment of urinary tract infections. Nitrofuran antibiotics and their metabolites are banned in the European Union because are considered mutagenic agents. Many nitrofuran antibiotics are slightly soluble in water and they are unstable under alkaline medium [32,33].

Sulfonamide antibiotics consist of a sulpha group attached to an amino group, in which sulpha and amino groups are substituted by organic cyclic groups conferring antibiotic properties. They are extensively used in animals. Sulfonamide antibiotics are stable molecules, insensitive to light and pH conditions and are excreted through urine as acetylated sulfonamides [34–36].

ANTIBIOTIC UPTAKE MECHANISMS

MOLECULAR INTERACTIONS BETWEEN ANTIBIOTICS AND ADSORBENTS

Water remediation for antibiotics using adsorbent materials occurs through chemical interactions well described for organic molecules. Those interactions depend on the antibiotic structure and the chemical structure of the adsorbent material as well. In general terms, the "like dissolves like" rule for interactions between a solute and a solvent can be applied to the interactions between a sorbent material and a molecule, becoming the *"like interacts like"* rule. Thus, the possible interactions between activated charcoal, biochar, or lignocellulosic materials and any antibiotic are:

1) Electronic dispersion interactions, also known as van der Waals or London forces, are weak interactions caused by electronic density fluctuations, which can be spontaneous or induced by the proximity of another molecule or chemical group present on a surface. Molecules with high electron density groups, such as instaurations and aromatic rings are prone to these types of interactions [38].

2) Dipole interactions are found in molecules with asymmetrical charge distribution due to the presence of functional groups comprising atoms with a higher electronegativity than the carbon or hydrogen atoms, such as oxygen, nitrogen, or halides. Those atoms attract electron densities towards themselves, generating a permanent uneven distribution of the electron density of a molecule. Interestingly, those dipole forces can induce electron density fluctuations in other molecules or chemical surfaces, interact with other dipoles, and/or charged (ionic) functional groups [38,39].

3) Hydrogen bonding interactions are observed in molecules with hydroxyl- or amino-containing groups, in which a hydrogen atom covalently bonded to a high electronegative group (hydrogen bond donor group) forms a bond with a second electronegative atom presenting a coordinating-electron par in their structure (hydrogen bond acceptor group). Hydrogen bonding interactions can be inter- or intra-molecular and are stronger than dipole interactions [38-41].

4) Ionic interactions are present in molecules with charged functional groups. Those charged groups interact through electrostatic attraction with ionic molecules or metal ions of opposite charge. Common ionic groups found in organic molecules and/or adsorbent materials include carboxylates, sulfonates, and ammonium groups [39-41].

Table 1 illustrates the general chemical structures of various antibiotic classes. Penicillins and cephalosporins can engage with sorbent materials through dipole, hydrogen bonding, and ionic interactions, attributed to the presence of carbonyl, amide, amino, and carboxylic acid groups. Aminoglycoside antibiotics form hydrogen bonds and ionic interactions due to their abundant hydroxyl and amino groups. Macrolide antibiotics primarily rely on hydrogen bonding and dipole interactions. Fluoroquinolones and tetracyclines exhibit interactions through dispersion, dipole, hydrogen bonding, and ionic forces due to their characteristic unsaturated and aromatic rings, as well as the presence of carbonyl, hydroxyl, and amino groups. Nitrofuran antibiotics engage in dispersion, dipole, hydrogen bonding, and ionic interactions, mainly due to instaurations in the furan ring, nitro groups, amide, and amino groups. Sulfonamide antibiotics interact primarily through dipole and hydrogen bonding, stemming from the sulfamide group.

BATCH STUDIES FOR ANTIBIOTIC UPTAKE

Generally, adsorption of antibiotics by static or batch mode (batch experiments) [42] allows obtaining significant data about the experimental factors that affect the adsorption of these contaminants in aqueous solution, such as pH of the medium, initial concentration of the adsorbate, contact time, temperature of the medium, among others [43]. Batch adsorption can be described from mathematical models of adsorption isotherms and kinetic models of adsorption, together with thermodynamic parameters [42-44], which allow us to explain the absorption mechanism produced between sorbent and adsorbate [43].

ADSORPTION ISOTHERMS

Adsorption is defined as a process of mass transfer (of an adsorbate) between the phases of a solid-liquid system, where the solid phase corresponds to the adsorbent and the liquid phase to the aqueous medium [42,45]. In this context, adsorption isotherms describe the relationship between the concentration of antibiotics retained by the adsorbents and the concentration of contaminant remaining in solution at equilibrium [42,44]. Moreover, the chemical nature of the sorbent used and the adsorbed antibiotic determine the resistance of the contaminant to being removed from the surface of the solid phase [42,45]. Various adsorption isotherms, mathematical models of one, two and three parameters are found in the literature, two-parameter models being the most commonly used [44,46]. Langmuir, Freundlich, Dubinin-Radushkevich, Temkin, Flory-Huggins, and Hill isotherms are defined by two-parameter models [44]. However, the Langmuir and Freundlich isotherms are widely preferred for the study of antibiotic absorption due to the convenience and clarity of their parameters and their ease of understanding [44,47,48].

The nonlinear expressions of the Langmuir and Freundlich isotherm models were evaluated using Equations 1 and 2, respectively.

$$q_e = \frac{q_{max} K_l C_e}{1 + k_l C_e} \qquad \textbf{Eq. 1}$$

$$q_e = k_f C_e^n \qquad \textbf{Eq. 2}$$

where q_e is the equilibrium adsorption capacity (mg g^{-1}), C_e is the equilibrium concentration of MB (mg L^{-1}), q_{max} is the maximum adsorption capacity (mg g^{-1}), k_l is the Langmuir constant (L mg^{-1}), k_F is the Freudlich constant, and $1/n$ is adsorption intensity.

The Langmuir model suggests that the surface of the sorbent has a fixed number of active binding sites with the same energy and affinity for the adsorbate [42]. This means that the solid phase's active sites only interact with the adsorbate, forming a monolayer on the material's surface (homogeneous surface) where the adsorbates do not interact with each other, and the adsorption is reversible [44]. When the Langmuir model accurately describes the experimental data, it's important to calculate the separation factor or equilibrium parameter (R_L) [44]. R_L is a dimensionless constant. When R_L equals 0, is less than 1, equals 1, or is higher than 1, it indicates an irreversible, favorable, linear, or unfavorable isotherm, respectively [44]. R_L is calculated using Equation 3:

$$R_L = 1/(1 + K_L C_0) \qquad \textbf{Eq. 3}$$

The Freundlich model assumes that the active binding sites on the surface of the material have different affinities for the adsorbate [42]. These sites interact with the adsorbate in order of affinity, with the sites having the highest affinity towards the adsorbate being occupied first [44]. Consequently, new active sites with a lower affinity (heterogeneous surface) are constantly generated, which are occupied by other adsorbates, thus forming a multilayer on the surface of the material [42] where the adsorbates can likely interact with each other [44]. The Freundlich equation is one of the first empirical models used to explain equilibrium data and adsorption properties on a heterogeneous surface [44]. The dimensionless Freundlich intensity parameter (n) is obtained from the mathematical model and indicates the heterogeneity of the adsorbent surface and the magnitude of the adsorption driving force.

KINETICS PARAMETERS

The contact time between adsorbate and adsorbent is another parameter that allows to elucidate the sorption mechanism [47,50]. Specifically, from these mathematical models, information such as the limiting reaction stage and the dependence of intra- or extra-particle diffusion phenomena on sorption can be extracted [44, 51]. There are several kinetic models, like Lagergren pseudo-first-order (PFO), pseudo-second-order (PSO), Avrami, Bangham, Boyd, Elovich, and intraparticle diffusion [51]. However, the most commonly used in antibiotic sorption studies are PFO, PSO, and Elovich [52-57].

The PFO and PSO models are generally used in liquid-solid sorption [51]. PFO indicates that mass transfer from the solution to the adsorbent surface is the limiting stage of the reaction [44]. PSO attributes that the determining step of the sorption kinetics is the chemisorption reaction [44]. Whereas the Elovich model postulates that the adsorption process resembles a chemical reaction, that is, as the amount of sorbate adsorbed in an adsorption system increases, the rate of adsorption decreases exponentially [57].

To elucidate this, the adsorbate-adsorbent contact time is compared as a function of qt, which is obtained with Equations 4-6 for PFO, PSO, and Elovich respectively [49-51].

$$q_t = q_e(1 - e^{-k_1 \cdot t}) \qquad \textbf{Eq. 4}$$

$$q_t = \frac{q_e^2 \cdot k_2 \cdot t}{1 + k_2 \cdot q_e \cdot t} \qquad \textbf{Eq. 5}$$

$$qt = \frac{1}{\beta} \cdot \ln(1 + \alpha\beta t) \qquad \textbf{Eq. 6}$$

where, qt (mg g^{-1}) indicates the amount of substance retained per unit mass of adsorbent at a specific time t (min), q_e (mg g^{-1}) represents the adsorbate retention at its equilibrium state, being the amount of substance adsorbed per unit mass of adsorbent when the sorption process has reached equilibrium, k^1 and k^2 (min^{-1}) are the retention constants of the respective models, β (mg g^{-1}) refers to the desorption constant, and α (mg g^{-1} min^{-1}) represents the initial rate constant [49-51].

To determine which model best fits the sorption phenomenon, the coefficient of determination (R^2) of the non-linear fit [49-51], in conjunction with the degree of applicability in terms of the sum of squared errors (SSE%), as shown in Equation 7 is used as a parameter [49].

$$SSE\ (\%) = \sqrt{\frac{\sum (q_{exp} - q_{e,cal})^2}{N}} \qquad \textbf{Eq. 7}$$

where N represents the number of data, q_{exp} is the experimentally obtained adsorption capacity (mg g^{-1}) refers to the amount of substance that was adsorbed per unit mass of adsorbent in the experiment, and $q_{e,cal}$ (mg g^{-1}) is the sorption capacity obtained from the linear regression of the kinetic model [58].

THERMODYNAMIC PARAMETERS

Thermodynamics can be effectively employed to investigate adsorption processes by performing serial adsorption experiments by varying the temperature and initial concentration and setting the optimum conditions, such as solute/liquid ratio, solution pH, and ionic strength [59]. Thermodynamic parameters can be determined when equilibrium is reached in adsorption [59]. These parameters are the change in Gibbs free energy (ΔG°), the change in enthalpy (ΔH°), and the change in entropy (ΔS°). The values of ΔG°, ΔH°, and ΔS° are derived from Equation 8 and can be plotted graphically by the Van't Hoff relationship, ln(Ke) versus 1/T, as described in Equation 9 [44]. These thermodynamic parameters provide information on the spontaneity of the adsorption process, the randomness, and the nature of the interaction between adsorbate and adsorbent [44].

$$\Delta G° = -R \cdot T \cdot ln\, K_c \qquad \textbf{Eq. 81}$$

$$\ln K_c = \frac{\Delta S}{R} - \frac{\Delta H}{RT} \qquad \textbf{Eq. 9}$$

where, T is the temperature in Kelvin (K) and R corresponds to the gas constant (J/(mol K)). Therefore, the equilibrium constant (Kc) must be dimensionless [44].

The accurate derivation of thermodynamic parameters depends directly on the equilibrium constant between two phases (Kc). Investigations have been reported

where the value of Kc can be determined from isothermal adsorption constants, such as Henry, Freundlich, Langmuir, Flory-Huggins, and Frumkin or from the partition coefficient [59,60].

ACTIVATED CARBON

AC can be defined as a carbonaceous and porous material. It is a predominantly amorphous solid that has a high surface area and an internal surface that exhibits a broad pore size distribution. Pores can be classified into macropores, mesopores and micropores, being their size > 25 nm, 1 nm < 25 nm and < 1 nm respectively [61]. Micropores comprise more than 90% of the surface area of the AC, where most of the adsorption of polluting species occurs [61]. AC has in its structure carbon atoms, as well as functional groups (which are mainly oxygen and nitrogen), formed during the physical activation process resulting from the use of oxidizing agents such as oxygen, carbon dioxide, steam water or mixtures [62][63]. The physicochemical characteristics of AC have made them the most attractive and widely used adsorbents for water decontamination [61], since their chemical composition and high degree of microporosity, well-developed surface area, and large distribution of pore volumes and diameters allow its effective use in the capture of organic species from effluents and, more recently, to remove pharmaceuticals from wastewater [31,64].

In general, the surface properties of AC depend mainly on the type of physical or chemical process and the activating agent used in the activation of AC [62]. The physical activation that is carried out commercially is based on activating the AC by subjecting it to high temperatures, from 800 to 1100 °C in the presence of gases, such as atmospheric oxidizing agents described previously [63]. Despite being an eco-friendly method, it involves high energy consumption and long processing times [65]. Instead, chemical activation uses temperatures ranging between 400 and 900 °C [63]. The activation agents used make it possible to minimize the formation of highly viscous, liquid, or semi-solid substances, increasing the content of AC in the final product [63]. The use of chemical substances as activating agents allows the development of a porous surface with a greater distribution of pore sizes [63], increasing the specific area of the material and therefore the adsorption efficiency of the material [66]. Although it is true, that chemical activation works at lower temperatures compared to physical activation, reducing the associated energy and economic cost [67], the use of chemical substances as activating agents causes water contamination through the effluents generated in the washing stage of the AC obtained [63].

Based on the systematic study of the literature, it is perceived that quinolones, β-lactams, sulfonamides, TC, and nitrofurans are among the most studied emerging contaminants for water remediation with AC adsorbents. Below are some antibiotic adsorption studies found in the literature depending on the type of emerging contaminant.

REMOVAL OF QUINOLONE ANTIBIOTICS USING AC

Ciprofloxacin (CIP) belongs to the fluoroquinolones family, and it has been widely prescribed for medical treatments, targeting a range of bacterial species with broad-spectrum activity [68,69].

El-Shafey *et al*. conducted a study on the adsorption of CIP from aqueous solutions. They utilized AC derived from date palm leaflets through H_2SO_4 carbonization at 160 °C. The experimental results revealed that the Langmuir model provided a better fit to the equilibrium data compared to the Freundlich model. Furthermore, the adsorption process followed a pseudo-second-order (PSO) model, demonstrating a maximum adsorption capacity of 133 mg g^{-1} at 45.0 °C and pH 6.00. Thermodynamic analysis indicated that the adsorption process is both endothermic and spontaneous, with a ΔG° value of -2.21 kJ mol^{-1} at 45.0 °C [68]. Chandrasekaran *et al.* conducted a study on the use of acid -AC derived from Prosopis juliflora wood (PPJ) for the adsorptive removal of CIP [69]. The experimental results revealed that the maximum adsorption capacity of PPJ, determined by the Langmuir model, was 250 mg g^{-1} under the conditions of a fixed PPJ dosage of 1.00 mg mL^{-1} and an initial antibiotic solution concentration of 100 mg L^{-1} at pH 4.00. The recycling process of PPJ revealed that the adsorbent can be employed for up to four cycles. Furthermore, the simultaneous presence of cationic and anionic salts exhibited minimal influence on the adsorption of antibiotics on the surface of PPJ [69]. Huang *et al*. conducted a study on the adsorption of a combination of CIP and TC onto AC prepared from lignin using H_3PO_4 impregnation. Their findings demonstrated that lignin-AC served as an efficient adsorbent for the simultaneous removal of CIP and TC, following a PSO model. The adsorption equilibrium data exhibited a good fit with the Langmuir isotherm, revealing maximum adsorption capacities of 476 mg g^{-1} for TC and 419 mg g^{-1} for CIP, respectively. Moreover, thermodynamic investigations demonstrated that the adsorption process was both spontaneous and favourable [70]. Bello et al. conducted a study on the adsorptive removal of CIP from aqueous media using AC derived from banana stalk (BSAC). In their research, they employed H_3PO_4 as a modification agent for the adsorptive material. The experimental results indicated that the maximum adsorption of 49.7 mg g^{-1} at 50.0 °C, optimized at pH 8.00 was best described by the Langmuir isotherm. Notably, it was observed a favourable interaction between the BSAC surface and CIP molecules in their zwitterionic form. The authors also provided evidence to support the thermodynamic preference of CIP sorption onto BSAC, with a ΔG° value of -6.27 kJ mol^{-1} [71]. Guellati et al. employed bamboo-based AC dispersed with aluminium to optimize the adsorptive removal of CIP antibiotics. Through their research, they determined that the adsorbent achieved a maximum CIP adsorption efficiency of approximately 93.6% (13.4 mg g^{-1}) when using an $AlCl_3$ concentration of 2.00 mol L^{-1} at pH 7.90, 25.0 °C and an adsorbent dosage of 3.00 mg mL^{-1} [72]. Alacabey conducted a study using AC derived from pumpkin seed shells that were modified with KOH as an adsorbent for the removal of CIP from aqueous systems. The maximum adsorption capacity, determined by fitting the Langmuir isotherm model was found to be 885 mg g^{-1} at pH 8.00. Thermodynamic analysis indicated that the adsorption process is both endothermic and spontaneous, with a ΔG° value of -5.72 kJ mol^{-1} at 30.0°C [73]. Sousa et al. investigated the use of microporous AC obtained from microwave pyrolysis of spent brewery grains for the adsorptive removal of antibiotics, including CIP. Their research revealed that the AC adsorbent exhibited optimal performance with a K_2CO_3:precursor ratio of 1:2 at 800°C. Without adjusting the pH, the adsorbent achieved a maximum Langmuir adsorption capacity of 206 mg g^{-1} for CIP at 25.0 °C [74]. Ahmed et al. produced granular activated carbon (KAC) by carbonizing Phoenix dactylifera L stones and subsequently subjecting them to microwave K_2CO_3 activation. They investigated the adsorptive removal of CIP and norfloxacin (NOR) using the KAC adsorbent. The results showed that the data best fit the Langmuir-type isotherm and second-order kinetics, as confirmed by the Thomas and Yoon-Nelson models. The q_0 parameters of the Thomas model for CIP and NOR on KAC were found to be 2.09 mg g^{-1} and 1.99 mg g^{-1}, respectively. This suggests a higher adsorption capacity of CIP compared to NOR, potentially due to CIP's higher water solubility and lower molecular weight [75]. Hrbáč et al. conducted a study on the utilization of activated carbons (ACs) derived from various agricultural waste biomasses, including red mombin seeds, corn cob (CC), coffee husk, internal and external parts of mango seeds, and ice cream beans. The ACs were prepared through conventional pyrolysis at 600 °C under a nitrogen atmosphere and activated with $ZnCl_2$. The aim was to investigate their efficacy in removing antibiotics such as NOR and ofloxacin (OFL) from water. The results indicated that all the investigated ACs exhibited strong adsorption of NOR and OFL. The adsorption kinetics were best described by the Elovich model, while the adsorption isotherms correlated well with the Redlich-Peterson model. The AC derived from red mombin seeds (RMS-based AC) demonstrated the highest adsorption uptake, with maximum adsorption capacities of 404 mg g^{-1} for NOR and 380 mg g^{-1} for OFL, as determined by Langmuir's model [76]. Zhang et al. conducted a study on the adsorptive removal of NOR from aqueous media using AC derived from keratin waste sources, specifically animal hairs (AHAC). They compared its physicochemical characteristics and sorption properties with AC derived from lignocellulose, specifically cattail fibers (CFAC). The adsorbents were impregnated with H_3PO_4 and then carbonized at 500 °C, resulting in materials with a combination of micropores and mesopores. The sorption kinetics and isotherms of NOR exhibited a good fit with the PSO model and Freundlich model, respectively. Furthermore, when the adsorbent surface area was normalized, the sorption of NOR onto AHAC was significantly higher compared to CFAC. This difference in sorption behavior was attributed to their distinct physical and chemical characteristics [77].

REMOVAL OF B-LACTAM ANTIBIOTICS USING AC

As mentioned above, amoxicillin (AMX) belongs to the β-lactams family and is widely used to control various respiratory tract infections in humans and used in veterinary medicine as a growth-enhancing and stimulating agent animal [78,79]. Joghtaei et al. conducted a study on the adsorption of the AMX antibiotic using AC derived from Azolla filiculoides. The AC was impregnated with $ZnCl_2$

and subsequently calcined at 600°C under a nitrogen atmosphere. The research findings indicated that the sorption data were effectively correlated with the PSO kinetic model and the Langmuir isotherm model. According to Langmuir's model, the maximum adsorption capacity was determined to be 265 mg g^{-1} at pH 7.00 [54]. Berges et al. conducted a study utilizing powdered AC derived from plants as an adsorbent for AMX. The research revealed a maximum adsorption capacity of 80.4 mg g^{-1}, with a contact time of 20.0 min between the adsorbent and the adsorbate. The adsorption process was found to be favoured in an acidic medium. The adsorption equilibrium data for AMX demonstrated a good fit with a Freundlich-type isotherm [81]. Furthermore, it was demonstrated that the interactions between the π orbitals of AMX and the adsorbent material may significantly contribute to the adsorption efficiency of AMX [81]. From the work of Chandrasekaran et al., the removal of AMX was also examined using the acid-AC prepared from PPJ [69]. The maximum adsorption capacity of PPJ for the AMX antibiotic, as determined by the Langmuir model, was found to be 714.3 mg g^{-1}. Additionally, a binary adsorption system consisting of both CIP and AMX was studied to evaluate any synergistic or antagonistic effects between the two antibiotics. To analyze the adsorption capacity of individual antibiotics in the binary system, a competitive Langmuir model was employed. The results indicated an adsorption capacity of 370.4 mg g^{-1} for CIP and 482.1 mg g^{-1} for AMX, confirming that CIP had an antagonistic effect on the adsorption of AMX, while AMX had a synergic effect on the adsorption of CIP on the surface of PPJ [69]. In their study, Hashemzadeh *et al.* investigated the effectiveness of acid-AC derived from Aloe Vera leaves (Av) for the removal of AMX from aqueous solutions. They further activated the AC using H_2SO_4 (Av-S-Ac) and HNO_3 (Av-N-Ac) separately. The researchers found that the experimental data exhibited a strong correlation with both the PSO kinetic model and the Langmuir isotherm model. The maximum adsorption capacity of AMX was observed at pH 3.00, resulting in 28.9 mg g^{-1} and 29.1 mg g^{-1} for the (Av-S-Ac) and (Av-N-Ac) adsorbents, respectively [82]. Ali *et al.* conducted a study on the utilization of zero-valent iron nanoparticles coated AC obtained from pomegranate peel (AC-nZVI) as an adsorbent for the removal of AMX from aqueous solutions. They optimized the conditions for maximum efficiency, achieving a removal efficiency of 97.9%. The optimal conditions included an AMX concentration of 10.0 mg L^{-1}, an adsorbent dose of 1.50 g L^{-1}, and a pH 5.00. The adsorption equilibrium data were fitted to the Langmuir monolayer isotherm model, which indicated a maximum capacity uptake of 40.3 mg g^{-1}. The kinetics of the adsorption process were well described by the pseudo-first-order (PFO) model [83].

REMOVAL OF SULPHONAMIDES AND TRIMETHOPRIM USING AC

SNs are one of the oldest and most widespread antibacterial drugs prescribed around the world. SNs can cause various unfavorable side effects, including diseases of the digestive and respiratory tracts, and they are not readily biodegradable [84]. Trimethoprim (TMP) is usually commercialized as a combined drug with SNs to treat or prevent urinary tract infections [1].

Fan et al. prepared AC from agricultural waste for the treatment of antibiotics-loaded wastewater. Cornstalk was used as a precursor to make a granular AC adsorbent for the removal of sulfamethoxazole (SMX) from water. The experimental kinetic data were adjusted to the PSO model, while the adsorption equilibrium data followed the Langmuir model, reaching a maximum adsorption capacity of 36.9 mg g^{-1} [85]. In other research, Jaria *et al.* studied the adsorption of SMX from buffered solutions and real wastewater samples, using AC derived from paper mill sludge (AC-P) and modified with thiol groups (AC-MPTMS). The adsorption data obtained were better described with the Langmuir isotherm, showing a maximum absorption of 113 mg g^{-1} for AC-P and 140 mg g^{-1} for AC-MPTMS at 15.0 °C and a pH of 8.00. The kinetics studies were best correlated to a PSO model. The thermodynamic parameters for both adsorbents showed the following values, $\Delta G°$ = -33.2 kJ mol^{-1} for AC-P and -26.4 kJ mol^{-1} for AC-MPTMS, indicating in both cases an endothermic adsorption process and spontaneous. Removal of SMX in real wastewater systems showed a lower performance using AC-MPTMS as the adsorbent material (q_m = 16.1 mg g^{-1}) explained by competitive matrix effects [86]. In addition, Hu et al. worked with a bagasse-derived AC (BAC-600) prepared and activated by one-step carbonization for SMX adsorption from aqueous media. Based on the Langmuir model, BAC-600 under controlled conditions at pH = 3.00 and T = 35.0 °C achieved a maximum SMX removal capacity of 215 mg g^{-1}. Additionally, it was found that the adsorption process was adjusted to the PSO model, and, from the thermodynamic studies, an endothermic and spontaneous process was corroborated ($\Delta G°$ = -4.74 kJ mol^{-1}). Reuse tests showed that after the fifth cycle, BAC-600 maintained a high adsorption efficiency of 190 mg g^{-1} [87]. It was found that the adsorption phenomenon is based on a combination of several mechanisms, being these interactions of the electrostatic type, hydrogen bonds and π-π interactions as shown in Figure 1.

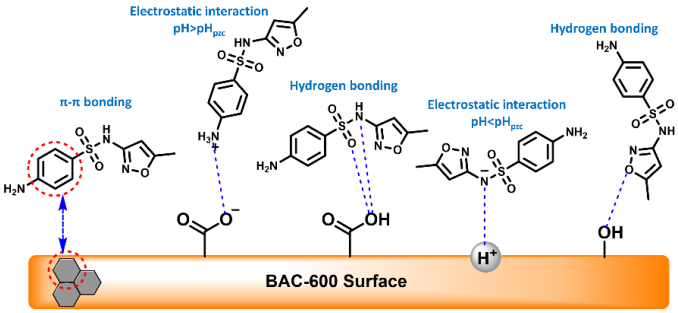

Figure 1. Schematic representation of the interactions presented in the phenomenon of SMX adsorption in BAC-600 [87].

Akhtar et al. studied the adsorption properties of a commercial AC from palm kernel shells (PAC) and modified with Fe_2O_3/CeO_2 (MOPAC) for SMX. The values obtained from the adsorption kinetic studies were fitted to the PSO model, while the adsorption equilibrium data followed the Langmuir isotherm model. Using the experimental conditions of 2.00 g L^{-1}, the initial pH ~6.50, and the contact time = 50.0 min for the adsorption studies. Catalytic degradation tests were also performed in the presence of MOPAC/O_3. The catalytic results showed that SMX was completely decomposed within 15.0 min of ozonation. Interestingly, SMX removal was higher with MOPAC/O_3 compared to PAC/O_3 at pH = 3.50 [88]. Sousa *et al*. also studied the removal of SMX and TMP using AC from spent brewery grains activated with K_2CO_3. Maximum Langmuir adsorption uptake of 217 mg g^{-1} for SMX and 229 mg g^{-1} for TMP were obtained, showing a better performance compared to the CIP antibiotic (206 mg g^{-1}) at the same optimized conditions [74]. Berges *et al.* not only studied the adsorptive removal of AMX, but they also assessed sulfadiazine (SDZ) and TMP antibiotics from an aqueous solution using the same vegetal powdered AC. The overall study indicates that SDZ and TMP demonstrated a higher affinity for the adsorbent compared to AMX. This observation can be partially attributed to their structural characteristics, which enable them to establish stronger π-π interactions with the adsorbent. Moreover, the sorption isotherms of TMP followed the Langmuir model, while SDZ fitted with both the Langmuir and Freundlich models. The kinetics studies of both compounds were fitted to the PSO model. Similarly, to AMX, sulfadiazine showed higher uptake under acidic conditions. In contrast, TMP adsorption was favoured in alkaline conditions [81]. Teixeira *et al.* conducted a study on the elimination of SMX using AC derived from walnut shells. The kinetics of adsorption was suitably described by a second-order polynomial equation. The pH level significantly influenced the removal efficiency of SMX, with the maximum capacity observed at pH 5.50. According to the Langmuir model, the maximum adsorption capacity was determined to be 107 mg g^{-1} [89].

Askari *et al*. synthesized AC from walnut wood and magnetized it with $CoFe_2O_4$ nanoparticles to improve the removal of cephalexin (CFX) from water. The equilibrium adsorption process and kinetics were investigated, revealing that the CFX adsorption process adhered to the Freundlich isotherm model and PSO kinetics. The optimal conditions for CFX removal were achieved at pH = 3.00, time = 30.0 min, antibiotic concentration = 50.0 mg L^{-1}, and adsorbent dose = 2.00 g L^{-1}, resulting in a K_f value of 21.7 mg L^{-1}[90]. In a different study, Theydan *et al*. prepared two types of AC from agricultural waste. Microwave treatment was applied to Albizia lebbeck seed pods, which were then activated using KOH KAC and K_2CO_3 (KCAC). These ACs were employed for the adsorptive removal of CFX, and their sorption properties were compared. The equilibrium isotherm data were found to fit well with the Langmuir-type isotherm, yielding maximum adsorption capacities of 137 and 118 mg g^{-1} for KAC and KCAC, respectively. The kinetic studies demonstrated a good correlation with the PSO model for adsorption onto both types of carbons [91]. In another research, Pouretedal and Sadegh produced carbon nanoparticles from Vinewood for the adsorption of AMX, CFX, TC, and PNG. The achieved adsorption efficiencies ranged from 74.0% to 88.0% after 8.00 h of contact [92].

REMOVAL OF NITROFURANS USING AC

Several nitrofuran antibiotics are currently on the market since they are used to treat several diseases such as topical infections, urinary tract infections, bacterial diarrhoea, and *Helicobacter pylori* infections among others [93]. For this reason, it has been detected in wastewater hospital effluents, constituting a potential risk for aquatic and terrestrial organisms. Ahmed *et al*. worked with *Siris* seed pods for the preparation of microporous AC using microwave-assisted activation in the presence of K_2CO_3 and investigated its sorption properties for the removal of metronidazole (MNZ), a nitroimidazole antibiotic from the family of nitrofurans. It was found that the adsorption data of MNZ has the best correlation with the Langmuir isotherm, showing a maximum sorption capacity of 181 mg g^{-1}. The kinetic studies showed the adsorption of MNZ on this AC follows a PSO kinetic model. Thermodynamic parameters from the MNZ sorption in this AC showed a spontaneous and exothermic process (ΔG° = -7645 kJ mol^{-1} at 30.0 °C)[94]. Teixeira et al. have also studied the adsorptive removal of MNZ by using the same walnut shell-based AC employed for the removal of SMX [89]. They found that with increasing pH, the removal of MNZ increases, with an optimal value of pH 8.00. The maximum uptake adsorption for MNZ following Langmuir´s model was 107 mg g^{-1} at 30.0 °C showing a better uptake performance compared to SMX (93.5 mg g^{-1})[89]. Ebili *et al*. conducted a study on the adsorption properties of an AC developed from carbonized tea leaves and modified with potassium hydroxide (TWAC). The aim was to remove MNZ from aqueous solutions. The equilibrium adsorption data exhibited good agreement with the Freundlich isotherm model, while the kinetic studies followed a PSO model. Thermodynamic analysis indicated that the adsorption of MZN onto TWAC is an exothermic and spontaneous process (ΔG° = -13.8 kJ mol-1 at 40.0 °C) [95]. Manjunath *et al*. synthesized AC using PPJ as a precursor and investigated its adsorptive properties for MNZ removal in a fixed-bed adsorption column. The breakthrough curves were analyzed, and the results demonstrated that the Thomas model provided a good fit for MNZ removal. According to the Thomas model, the maximum adsorption uptake was 9.70 mg g^{-1} for MNZ. The researchers also examined a multi-component system comprising MNZ with PO_4^{3-} and NO_3^-. The results indicated that the multi-component system exhibited antagonistic behaviour in sorption, resulting in an adsorption capacity approximately 2.50 times lower (3.94 mg g^{-1}) than that of the mono-component MNZ system [96].

Table 1 details a summary of the studies of adsorption of emerging contaminants by AC that were found through the systematic study of the literature and details the maximum capacity of adsorption based on different experimental variables.

Table 1. Summary of adsorption results of organic pollutants by AC.

Material	**Antibiotic**	**Concentration** (mg L^{-1})	$\mathbf{Q_{max}}$ (mg g^{-1})	**pH**	**T** (ºC)	**R** (%)	**Ref.**
Palm leaflets AC	CIP	100	133	6.0	45	--	[68]
PPJ AC	CIP	100	250 m g^{-1}	4.0	30	98.8	[69]
Lignin-AC	CIP	400	419	5.5	20	--	[70]
BSAC AC	CIP	50	49.7	8.0	50	--	[71]
Bamboo-AC	CIP	50	13.4	7.9	25	93.6	[72]
Pumpkin seed shells AC	CIP	100	885	8.0	45	99.0	[73]
Spent brewery grains AC	CIP	7.36	206	Not adjusted	25	--	[74]
Phoenix dactylifera L stones AC	CIP	150 Fixed bed	2.00	Not adjusted	30	--	[75]
Agricultural waste AC	NOR	125	404	Not adjusted	23	--	[76]
Agricultural waste AC	OFL	250	380	Not adjusted	23	--	
Keratin waste AC	NOR	31.9	311	6.5	25	99.0	[77]
Azolla filiculoides AC	AMX	100	265	7.0	25	90.0	[80]
PPJ AC	AMX	100	714	6.0	30	80.3	[69]
Aloe Vera leaves AC	AMX	50.0	29.0	3.0	25	95.4	[82]
Pomegranate peel AC	AMX	10.0	40.3	5.0	25	97.9	[83]
Cornstalk AC	SMX	100	36.9	7.0	25	95.0	[85]
Paper mill sludge	SMX	5.00	113	8.0	15	--	[86]
Bagasse AC	SMX	100	215	3.0	35	--	[87]
MOPAC AC	SMX	80.0	65.9	6.5	30	--	[88]
Spent brewery grains AC	SMX	5.00	217	Not adjusted	25	--	[74]
Spent brewery grains AC	TMP	5.80	229	Not adjusted	25	--	[74]
Vegetal powdered AC	AMX	15.0	80.4	4.0	25	40.0	[81]
	SDZ		137	6.0		67.0	
	TMP		126	6.0		48.0	
Walnut shell-based AC	SMX	10.0	107	5.5	30	--	[89]
Walnut wood $CoFe_2O_4$	CFX	50.0	42.4	3.0	25	96.8	[90]
Albizia lebbeck seed pods KOH AC	CFX	100	137	7.0	50	--	[91]
Carbon NPs from Vinewood Activated with NaOH	AMX	20.0	2.69	2.0	25	55.6	[92]
	CFX		7.08			76.0	
	TC		1.98			88.2	
	PNG		8.41			73.9	
Siris seed pods AC	MNZ	100	181	7.0	30	--	[94]
Walnut shell-based AC	MNZ	40.0	127	8.0	30	--	[89]
Tea leaves KOH AC	MNZ	100	188	7.0	30	--	[95]
PPJ AC	MNZ	100 Fixed bed	9.70	Not adjusted	25	--	[96]
Lignin AC	TC	400	476	5.5	20	--	[70]

BIOCHAR

Biochar (BC) is a solid material derived from biomass carbonization under oxygen-limited conditions. It serves as a precursor to AC and has recently shown promising potential for adsorbing both inorganic and organic pollutants from aqueous and soil systems [18]. Various materials, such as agricultural and forest residues, industrial by-products or wastes, and unconventional materials from food and animal manures can be used as precursors for producing BC [17]. Consequently, the properties of BC are greatly influenced by the type of precursor and carbonization conditions [64]. The main advantage of BC over activated carbon is its lower production cost, as it can be manufactured without the need for higher temperatures and additional activating agents that are often required for AC production [64].

REMOVAL OF QUINOLONE ANTIBIOTICS USING BC

Li et al. reported the use of spent tea leaves as a precursor to obtaining BC (UTC), capable of removing CIP from aqueous media. This BC was prepared by pyrolyzing the precursor at varied temperatures to obtain spent tea leaf BC with a maximum adsorption capacity of 238 mg g^{-1}. Is is due to the presence of -OH groups, aromatic ring conjugations and C=O bonds on the surface of the BC, fitting Langmuir and PSO isotherm and kinetic models, respectively [99]. In addition, Zeng *et al*. [74] used rice husks (RH) as a precursor to obtain a BC for CIP removal, where it was corroborated that increasing carbonization temperature of the BC also increases the adsorption capacities of the material due to higher surface area and pore volume. The maximum adsorption capacity was 36.1 mg g^{-1}, due to the chemical interaction between the oxygen-containing functional groups of the BC surface, involving phenolic -OH and OR' alkoxy. Those groups interact with the amine groups of the CIP [100]. Li *et al*. [101] used sewage sludge and bamboo waste as precursors and BC, obtaining a high CIP removal efficiency of 95.0% and with an adsorption capacity up to 62.5 mg g^{-1}, fitting the Langmuir isotherm model. Likewise, this situation is reported when using banana peels as a precursor, showing that the maximum adsorption of antibiotics is achieved with the BC pyrolyzed at 750 °C in which the smallest particle size was obtained. The maximum CIP uptake was 23.3 mg g^{-1} at 10.0 °C following the Langmuir isotherm model [102]. Animal-derived BC was studied for the removal of CIP [77]. The BC was obtained from meat and bone meal (MBM) carbonized at 500 °C. It was found, by the surface characterization, that MBM biochar contains abundant oxygen moieties such as ether groups and hydroxyl groups, in contrast to the plant-derived BCs that usually contain less oxygen[103]. However, the maximum uptake of CIP was 14.4 mg g^{-1} according to the Langmuir isotherm model and PSO kinetics.

The adsorptive removal of antibiotics has been also studied for modified BCs. Hu *et al.* conducted a study in which they produced a novel magnetic BC by modifying camphor leaves with ZnO nanoparticles for removing CIP [104]. The material underwent calcination at 650 °C, resulting in a microporous structure with a significant surface area of 915 m^2 g^{-1}. The adsorption equilibrium data were well-matched with the Langmuir isotherm model, and the maximum adsorption capacity for CIP was found to be 449 mg g^{-1} at 40.0 °C. In addition, recycling studies showed that the adsorption performance did not decline after three times regeneration. Since the sorption properties of modified BCs are enhanced compared to unmodified BCs (due to the creation of more adsorption sites), in recent years, other research related to this area has also been reported, such as the novel Fe_3O_4/graphene oxide/citrus peel-derived BC (mGOCP) developed by Zhou *et al* for the removal of CIP [105]. A hierarchically porous magnetic bio-nanocomposite (mGOCP) was synthesized using a simple one-pot hydrothermal method. Among the different compositions tested, the mGOCP-1% (w/w mCP-GO = 1.00%) exhibited superior adsorption performance with a maximum adsorption capacity of 283 mg g^{-1} for CIP. The adsorption mechanisms for CIP were found to be governed by various interactions, including π-π electron donor-acceptor interaction, H-bonding, hydrophobic interaction, and electrostatic interaction, indicating a strong affinity between the adsorbent and the antibiotic. Additionally, it was observed that by incorporating graphene oxide (GO), the surface morphology and structural composition of BCs could be controlled, leading to an improvement in the antibiotic adsorption capacity [105]. Sayin et al. [80] worked with a BC produced from *Prunus cereus* waste stalk and modified with H_3PO_4 (MPCWSB) to remove CIP antibiotic from water solution. Analogous to the un-modified BCs, the adsorption efficiency of MPCWSB pyrolyzed at different temperatures was enhanced by increasing the carbonization temperature. The highest removal efficiency was achieved with BC that underwent pyrolysis at 500 °C referred to as MPCWSB500. The adsorption of CIP was evaluated using different kinetics and isotherm models, revealing a maximum adsorption capacity of 410 mg g^{-1} based on the Langmuir isotherm model. These results were obtained under optimal experimental conditions, including a pH value of 6.30, a contact time of 40.0 min, and a dose of 15.0 mg of MPCWSB500. To compare the benefits of BC modification for the adsorptive removal of CIP, Li et al. prepared BCs using potato stems and leaves [107]. The unmodified BC was synthesized by pyrolysis at 500 °C under anaerobic conditions (PB), while the modified BC was treated with a KOH solution (alkali-modified BC-APB). It was found that the alkali-treated BC (APB) has more mesopores than raw BC (PB), hence, exhibiting a better adsorption capacity (23.4 mg g^{-1}) than PB (8.48 mg g^{-1}) concluding that BC modifications are beneficial for the adsorption capacity of raw BC. In one study, Egbedina *et al*. also compared the adsorption properties of raw BC derived from coconut husk and kaolinite modified with $ZnCl_2$ (KCB) and further activated with HCl (KCB- and KOH (KCB-B) for the adsorption of CIP from water solutions [108]. Based on the Langmuir isotherm model, the maximum adsorption capacities were determined to be 71.0, 140, and 229 mg g^{-1} for KCB, KCB-A, and KCB-B, respectively. The improved adsorption performance of KCB-A and KCB-B can be attributed to an increase in the availability of active adsorption sites. In addition, Hamadeen et al. conducted a study on the sorption properties of nanostructured activated BC (nPPAB) derived from pomegranate peels (PP) for the removal of CIP [109]. In this research, pomegranate peels were carbonized at 800 °C and activated using H_3PO_4. The equilibrium and kinetic data exhibited good agreement with the Langmuir isotherm model and a PSO model, respectively. The maximum adsorption capacity of CIP was found to be 143 mg g^{-1} for nPPAB, whereas the bulk PP showed a maximum CIP adsorption of 5.92 mg g^{-1}, indicating the enhanced sorption properties of the modified BC. The investigation of the adsorption removal mechanism of CIP by nPPAB revealed the simultaneous occurrence of four removal pathways: π-π interaction (1), hydrogen bonding (2), electrostatic interactions (3), and hydrophobic interaction between nPPAB and CIP (4) (see Figure 2).

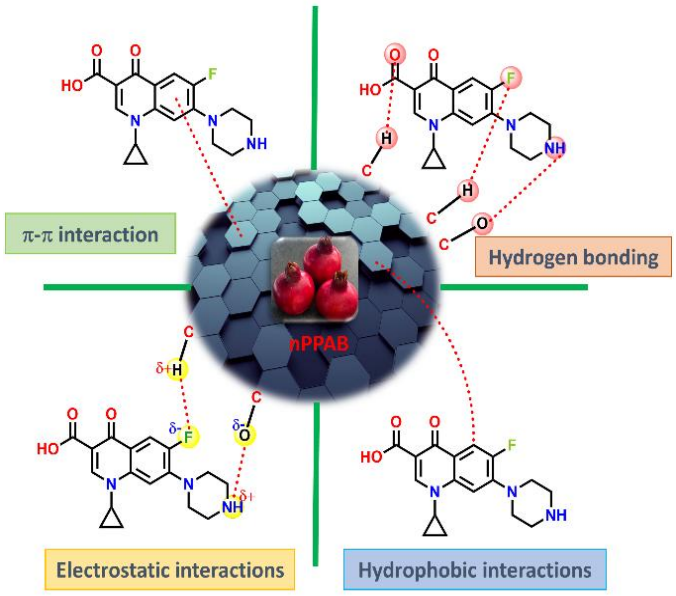

Figure 2. Schematic representation of CIP removal pathways by nPPAB [109].

As an attempt to improve the sorption capacity of BC derived from brown seaweed (*Sargassum crassifolium*) (SWBC), Atugoda et al. modified SWBC with zeolites to remove CIP (zeolite: BC = 1:5; SWBC-Z) [110]. The maximum adsorption capacity following the Langmuir isotherm model for unmodified SWBC was 34.4 mg g^{-1}, while the modified one reached 93.7 mg g^{-1}, showing an evident increment of the adsorption capacity due to the improvement of the active surface sites by modification with zeolites. Brønsted acid sites containing ≡Si–OH–Al≡ groups on zeolites are responsible for the enhanced sorption properties of the modified BC by the electrostatic attractions and hydrogen bonds can be formed between polar functional groups of CIP and SWBC-Z in the pH range of 6.50 – 8.00 as shown in the Figure 3 [110].

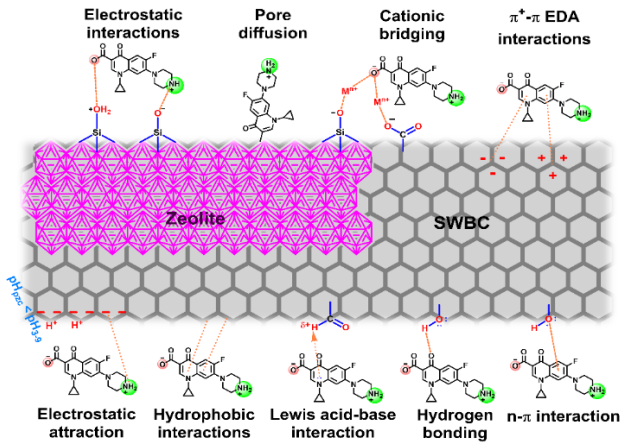

Figure 3. Schematic representation of various interaction mechanisms between CIP and SWBC or SWBC-Z adsorbents [110].

In another study, BC derived from brown seaweed (*Ascophyllum nodosum*) was hydrothermally carbonized and activated with $ZnCl_2$ (HTC-$ZnCl_2$) for the removal of CIP from water [111]. It was found that HTC-$ZnCl_2$ BC achieved good adsorption performance in a wide range of pH conditions. Using the optimized conditions, the maximum adsorption was to be around 400 mg g^{-1} and fit the Langmuir isotherm model.

Subsequently, Wu *et al*. assessed the adsorption performance of N-doped CC-derived BC for removing NOR antibiotics from aqueous media [112]. In this study, urea N-doped BC (U-MBC) was synthesized by the ball-milling method. The results exhibited a higher adsorption capacity for NOR using U-MBC (11.5 mg g^{-1}) which was almost four times higher than pristine BC (2.83 mg g^{-1}) between pH 3.00 and 9.00, enhanced adsorption was explained due to the formation of hydrogen bonds, possible π-π electron donor-acceptor interaction and pore-filling interactions resulting from the N-doping method [112].

REMOVAL OF SULFONAMIDE ANTIBIOTICS USING BC

BCs from different feedstocks can dramatically change their adsorption performance for the removal of antibiotics, although it is still unclear how the BC composition affects the adsorption properties. In this context, Wan et al. studied the adsorption of sulfamethazine antibiotic (SMZ) from water solutions, using the components of the lignocellulosic biomass [113] concluding that the SMZ adsorption behavior of BCs is related to their physicochemical characteristics. In the case of the lignin BC, no adsorption capacity was found due to the high ash content, while the xylan and cellulose BCs indicated dependence on the pH of the medium; however, xylan achieved a higher adsorption capacity. The adsorption mechanism study indicated that the process is governed by electrostatic repulsion, π-π (EDA) interactions, and hydrogen bonds as shown in Figure 4[113].

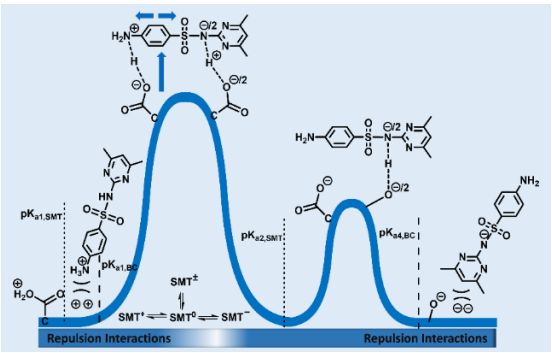

Figure 4. Proposed adsorption mechanism for SMZ on BCs at different pH values. The blue band at the bottom represents changes in electrostatic repulsion [113].

Cotton shell-derived BC activated with phosphoric acid was used for the adsorptive removal of sulfadiazine antibiotic (SDZ) [114]. Phosphoric acid is used to activate BC, derived from cotton hulls by pyrolysis, to improve its sulfadiazine (SDZ) adsorption capacity. Various impregnation ratios and times were studied to determine the optimum conditions. The best performance for SDZ removal was achieved with a pyrolysis condition of 2.50 impregnation ratio and 6.00 h impregnation time. At 298 K, the maximum adsorption capacity was 86.9 mg g^{-1}. The adsorption process of SDZ by BC was investigated using the PSO model, and the experimental data were well described by Langmuir and Temkin isotherms at different temperatures. The adsorption of SDZ was determined to be an exothermic process based on thermomechanical analysis. In addition, activated BC demonstrated recyclability for SDZ removal, with a high removal rate for at least five cycles. Therefore, activated BCs show great potential as effective adsorbents for SDZ removal. Sun *et al*. claimed that BC is a low-cost adsorbent for adsorptive removal of antibiotics from wastewater, but the adsorption efficiency still needs to be improved [115]. In this context, they prepared a coconut shell BC activated with KOH to enhance the adsorption efficiency and it was magnetically modified with $FeCl_3$ to enable its recycling. The magnetized activated BC was used for the adsorptive removal of a series of sulfonamide antibiotics (SA). The maximum adsorption capacities for SDZ, SMZ and SMX were 294, 400, and 455 mg g^{-1}, respectively, between five and seven times higher than those achieved with crude BC. It was observed that SAs were adsorbed on the modified BC via hydrogen bonds between SA molecules and the -OH/-COOH groups of BC. The results of adsorption kinetics and isotherms showed that the adsorption process follows a PSO kinetic model and a monolayer adsorption mechanism [115].

In order to improve the adsorption efficiency of antibiotic contaminants in water, Liu *et al*. developed hierarchical porous BC derived from onion skin with extremely high specific surface area (termed OHPBCs) [116]. This prepared OHPBC material demonstrated rapid adsorption equilibrium, achieving it in only 10.0 min, and exhibited a maximum adsorption capacity of 1281 mg g^{-1} for SDZ, which represents an outstanding result for sulfonamides removal. The adsorption process adequately fitted the PSO kinetic model and Langmuir isotherm model. Moreover, OHPBC could be regenerated and recycled up to three times without a significant decrease in its adsorption capacity.

Agricultural wastes like bagasse can also be used as feedstocks for preparing BC. In this regard, Wang et al. prepared BCs from bagasse with a washing treatment of acetone (BCA) and nitric-acid washing BC (BCN) to remove SMX from aqueous media [97]. The best performance was achieved with BCN with a maximum adsorption capacity for SMX of 275 mg g^{-1}, showing the potential of agricultural waste BCs to remove antibiotic pollutants.

One of the best performances on the removal of sulfonamides was achieved with activated porous BC derived from CC xylose residue reported by Li et al. [117]. In this study, BC was prepared and activated by KOH at 850 °C and used to remove SMX from aqueous solutions. The adsorption process on BC activated at 850 °C was rapid and highly efficient, achieving a maximum adsorption capacity of 1429 mg g^{-1}, a value notably higher than other BC adsorbents reported previously. This improved adsorption performance was attributed to the pore filling and π-π interaction, as well as the presence of a large surface area and abundant oxygen-containing functional groups on the surface of the BC activated at 850 °C.

To upgrade the notable performances of BCs for the removal of antibiotic pollutants, some researchers have modified BCs by adding catalysts for the oxidative degradation of organic molecules. In this regard, the study of Chu *et al*. deals with nickel-containing and nitrogen-doped BC (from balsa wood) (Ni@NBC) for the oxidative removal of sulfachloropyridazine (SCP) [118]. Under the optimized conditions, the Ni@NBC material exhibits a maximum adsorption capacity of 22.5 mg g^{-1} for SCP and could act as a catalyst to activate potassium persulfate (PPS) for the rapid and efficient degradation of SCP by an oxidative process (~ 90.0% within 30.0 min). The Ni@NBC also showed excellent reusability (>70.0 % degradation rate after 20.0 cycles), demonstrating that these materials have prospects in the application of remediation of aquatic environments.

Finally, based on the above, Table 2 shows a summary of the studies on the adsorption of quinolone and sulfonamide antibiotics by BC that have been reported in recent years detailing and comparing their maximum adsorption capacities as a function of different experimental variables, such as percussor, pH, and temperature.

Table 2. Summary of adsorption studies of organic pollutants by BC.

BC	Antibiotic	Concentration (mg L^{-1})	Q_{max} (mg g^{-1})	pH	T (°C)	R (%)	Ref.
Used tea leaves BC	CIP	250	238	6.00	40.0	---	[99]
Rice Husk BC	CIP	40.0	36.1	6.00	45.0	---	[100].
Sewage sludge-Bamboo BC	CIP	10.0	62.5	6.00	30.0	95.0	[101]
Banana peels BC	CIP	0.500 -100	23.3	3.00	10.0	---	[102]
Meat-bone meal BC	CIP	0.500 -100	14.4	5.00	25.0	---	[103]
Corncob BC	CIP	0.100 -1.20	0.40	Not adjusted	20.0	68.0	[104]
Camphor leaf-ZnO BC	CIP	100	449	4.00	40.0	---	[105]
Fe_3O_4/graphene oxide/citrus peel-BC	CIP	160	283	6.00	25.0	---	[106]
Prunus cereus waste BC	CIP	250	410	6.30	25.0	99	[107]
Potato steam and leaves BC	CIP	10.0	23.4	5.00	35.0	---	[108]
Kaolinite-coconut Husk BC	CIP	10.0 - 150	229	4.00	30.0	97.0	[109]
Pomegranate peel nano-BC	CIP	25.0	143	7.00	25.0	97.0	[110]
Brown seaweed-Zeolite modified-BC	CIP	10.0	93.7	6.50 - 8.00	25.0	---	[111]
Brown seaweed $ZnCl_2$ modified-BC	CIP	30.0	400	7.00	35.0	---	[111]
Corn stalk N-doped BC	NOR	5.00 – 50.0	11.5	7.00	25.0	89.0	[112].
Cellulose-based BC	SMZ	1000	---	6.50	25.0	---	[113]
Hemicellulose based BC	SMZ	1000	---	4.50	25.0	---	[113]
Cotton shell-derived BC	SDZ	10.0 - 100	86.9	4.00	25.0	---	[114]
Coconut shell BC modified with $FeCl_3$	SDZ	10.0 - 100	294	5.00	25.0	---	[115]
Coconut shell BC modified with $FeCl_3$	SMZ		400			---	
Coconut shell BC modified with $FeCl_3$	SMX	10.0 - 100	455	5.00	25.0	---	[115]
Onion skin-derived BC	SDZ	10.0 – 60.0	1281	4.00	25.0	---	[116]
Bagasse BC	SMX	200	275	4.00	25.0	---	[97]
CC xylose-derived BC	SMX	300	1429	Not adjusted	30.0	98.5	[117]
Balsa wood nitrogen-doped BC modified with Ni	SCP	20.0	22.5	7.00	25.0	---	[118]

LIGNOCELLULOSIC MATERIALS

The use of lignocellulosic materials (LM) has attracted increasing interest in the scientific research community due to their benefits, such as their sustainability and biodegradability [119]. LM stand out above the other materials presented in this review due to their great abundance, low economic cost and attractive structural and chemical composition that has numerous and diverse functional groups capable of interacting with pollutant molecules or that can be modified to improve its adsorption capacity [120]. LM is a sustainable raw material that can be extracted from various natural sources, such as trees, leaves, and agricultural residues (corncob), as well as forest waste, among others [120]. LMs are mainly composed of three different biopolymers; hemicellulose, cellulose and lignin and can be used as adsorbent materials [121].

CELLULOSE

Cellulose is the most abundant biopolymer in nature, it is biodegradable, biocompatible, non-toxic, and mechanically resistant. From cellulose, derivatives of interest can be obtained, such as microcrystalline cellulose, also known as purified cellulose [122]. Microcrystalline cellulose is used in the pharmaceutical industry as an excipient in the manufacture of tablets by compression and in powdered drugs and drug delivery [122], due to its interesting adsorbent-desorbent interaction with the drug in combination [123]. In addition, the properties of microcrystalline cellulose make it an attractive option for the removal of pharmaceuticals, such as antibiotics, from aqueous solutions.

Removal of antibiotics using cellulosic materials

El-Samaligy et al. reported in 1986 the investigation on the adsorptive-desorptive interactions of microcrystalline cellulose with ampicillin monohydrate (AMP) and AMX, formulated usually as a capsule and reconstitutable suspension forms [123]. The maximum adsorption uptakes for AMP and AMX, according to the Langmuir isotherm, were 87.7 and 18.5 mg g^{-1}, respectively. These findings provided important insights into the adsorption properties of cellulose and its potential application as an adsorbent for antibiotics. Over the past few years, cellulose has been subject to modifications and used as an adsorbent for the remediation of various organic pollutants, including dyes and, more recently, antibiotics. In relation to this, Feizi *et al*. developed a cellulose nanocrystal (CNC) derivative with carboxylalkylation, incorporating carbon chains of different lengths [124]. The material was thoroughly studied on the adsorption of doxycycline (DOX). Maximum DOX adsorption occurred at pH 6.00 when carboxypentadecanated CNC (PCNC) was used, which means that the CNC was carboxyalkylated with a longer carbon spacer. This was due to electrostatic and π interactions, as well as hydrogen bonding, as illustrated in Figure 5.

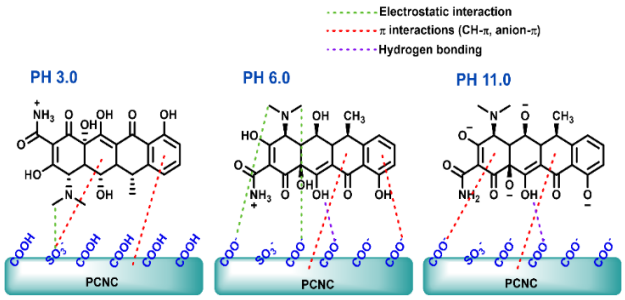

Figure 5. A schematic representation of the chemical interactions between DOX and PCNC at different pH values [124].

Yao et al. investigated a hybrid composite of cellulose nanofibrils and graphene oxide (CNF/GO) as an adsorbent to remove 21 kinds of antibiotics from water [125]. The CNF/GO adsorbent demonstrated outstanding adsorption

capacity towards different types of antibiotics, with the following adsorption efficiencies: TC > Quinolones > Sulfonamides > Chloramphenicols > β-Lactams > Macrolides. The adsorption values of the CNF/GO aerogel, according to the Langmuir model were 419 mg g^{-1} for chloramphenicol, 292 mg g^{-1} for macrolides, 128 mg g^{-1} for quinolones, 231 mg g^{-1} for β-lactamases, 227 mg g^{-1} for sulfonamides, and 455 mg g^{-1} for TC, demonstrating the efficiency of the modified cellulose composite for the removal of antibiotics from water.

Tao et al. also conducted research in which they developed an adsorbent material based on cellulose nanocrystals and graphene oxide (CNCs-GO) with three-dimensional structure to remove levofloxacin hydrochloride (LH) from water sources [126]. They determined the optimum conditions for LH adsorption, which included an initial contaminant concentration of 10.0 mg L^{-1}, an initial pH of 4.00, an adsorbent dosage of 0.1 g L^{-1} and a contact time of 4 h. According to their results, the suggested interaction mechanism between the LH and the adsorbent involves hydrogen bonds and electronic interaction, and the process is mainly governed by chemical adsorption behavior [126,127].

Following a similar direction of cellulose composites, Li et al. described the production of a composite material consisting of carboxylated cellulose nanofibers and montmorillonite (CMNFs-MMT), which was employed as an adsorbent for LH removal from river water and pure water solutions [127]. When comparing the equilibrium adsorption removal between pure water and river water, it was observed that the removal rate in river water (90.4%) was slightly lower than that in pure water (94.0%), suggesting that CMNFs-MMTs are relatively insensitive to environmental conditions.

Cellulose-based membranes present considerable potential in wastewater treatment. To explore this, Gao *et al.* developed hybrid laminated membranes composed of GO and cellulose nanocrystals (GO/CNC). These membranes were applied to the removal of two types of fluoroquinolones, NOR and LH [128]. The optimal removal efficiencies of GO/CNC toward the antibiotics were 90.9, and 97.2% for LH, and NOR, respectively.

Novel hybrid membranes based on these materials offer a promising approach to creating effective adsorbents for water purification.

Gopal et al. developed a new adsorbent material using carboxymethyl cellulose (CMC), acrylamide (AM) and Fe clay to efficiently remove CIP and LH antibiotics [129]. Hydrogel beads composed of this nanocomposite demonstrated a maximum adsorption capacity of 57.8 mg g^{-1} and 38.0 mg g^{-1} for CIP and LH, respectively, according to the Langmuir model. Reuse analysis indicated that the removal efficiency of CIP and LH remained above 85.0 % and 90.0 %, respectively, until the fifth cycle. Li et al. [130] synthesized composite aerogels (CMC-CG) using carboxymethyl cellulose and κ-carrageenan for adsorption removal of CIP in aqueous solutions. The maximum adsorption uptake of CIP was approximately 421 mg g^{-1} at pH 5.00. Cantero-López et al. developed a hydrogel using the vinyl monomer 2-methacroyloxyethyltrimethyl ammonium chloride (ClAETA) along with cellulose nanofibrils (CNF) to remove nafcillin (NAF). The adsorbent showed an adsorption capacity of 43.1 mg g-1 and 70.0% efficiency in removing NAF [131].

In another study, Hu et al. demonstrated the effectiveness of cellulosic materials in removing tetracyclines. They developed a composite utilizing bacterial cellulose and Ca-MMT for the removal of TC from wastewater [132]. The adsorbent exhibited a significant uptake capacity of 231 mg g^{-1} for TC based on the Langmuir isotherm model. Recycling experiments revealed that the system could be regenerated up to four times while maintaining its adsorption efficiency. In a similar way, Lu et al. synthesized iron(III)-loaded cellulose nanofibers (Fe(III)@CNFs) derived from bamboo to adsorb TC, chlortetracycline (CTC), and oxytetracycline (OTC) from water [133]. Fe(III)@CNFs demonstrated a maximum adsorption capacity of 294 mg g^{-1}, 233 mg g^{-1}, and 500 mg g^{-1} for TC, CTC, and OTC, respectively. Furthermore, recycling studies indicated that the TC adsorption capacity remained stable even after five cycles when the regeneration method involved UV+H_2O_2. This study highlighted the potential of Fe(III)@CNFs adsorbents for applications in antibiotic remediation.

In addition, Juengchareonpoon et al. investigated the application of graphene oxide and carboxymethylcellulose (GO-CMC) nanocomposites in citric acid crosslinked films for the efficient adsorption of OTC from aqueous solutions [134]. The maximum adsorption capacity for OTC was determined to be 102 mg g^{-1} based on the Langmuir isotherm model. Kinetics studies showed a good correlation with the PSO model. The prepared film could be easily regenerated through washing and reused for up to five cycles, highlighting the potential of these materials. In a related study, the same authors [135], reported the removal of OTC using hydrogel films composed of β-cyclodextrin/carboxymethylcellulose (β-CD/CMC). It was observed that the adsorption capacity of OTC depended on the active β-cyclodextrin content, with a maximum adsorption capacity of 27.2 mg g^{-1} at pH 8.00.

ALOthman et al. developed copper-carboxymethylcellulose nanoparticles to remove TC. Nevertheless, the maximum adsorption capacity achieved with these nanoparticles (1.11 mg g^{-1}) was found to be lower compared to other cellulose-derived materials, as indicated by the Langmuir isotherm model [136].

Abd El-Monaem et al. synthesized a composite material called UiO-66/ZIF-8/PDA@CA, which consisted of a zwitterionic UiO-66/ZIF-8 binary metal-organic framework (MOF) and polydopamine incorporated into cellulose acetate. The composite was in the form of floated beads and was designed for the removal of TC from water [137]. According to their findings, the maximum adsorption capacity of UiO-66/ZIF-8/PDA@CA was 291 mg g^{-1} at 25.0°C, as determined by the Langmuir model. Furthermore, the adsorption kinetics of TC onto the composite material were well-described by a PSO kinetic model. Pham *et al*. synthesized nanomaterials derived from RH that were modified with synthetic polydiallyldimethylammonium chloride. Their study demonstrated a maximum retention efficiency of 92.3% for AMX under specific conditions, including a contact time of 180 minutes, pH 10.0, and an adsorbent dose of 10.0 mg mL^{-1} [121]. Adsorption kinetics were fitted to the PSO model and determined that AMX removal is mainly controlled by electrostatic attraction [121]. Saldarriaga et al. developed an adsorbent from olive stone composed mainly of LM, with an adsorption efficiency of 95.0% when adsorbing AMX during 30.0 min of contact, with an initial adsorbate concentration of 200 mg L^{-1} and adjusting to PSO kinetics and a Langmuir isothermal model [138].

Similarly, Yang et al. developed nanocellulose-based materials for the removal of AMX and achieved a maximum retention capacity of 138 mg g^{-1}. The adsorption process was well-described by a PSO kinetic model and a Freundlich isotherm model [139]. Moreover, Sayen et al. investigated the sorption properties of a lignocellulosic substrate derived from wheat bran, which is an agricultural by-product, for the removal of enrofloxacin (ENR) antibiotic from water. The results demonstrated that the substrate could remove 100% of enrofloxacin within less than one hour at pH 6.00 [140]. The equilibrium data analysis revealed a good fit with the Sips model, suggesting heterogeneous monolayer adsorption of the antibiotic. The substrate exhibited a favourable maximum adsorption capacity of 91.5 mg g^{-1} at pH 6.00.

Table 3 summarizes adsorption studies using cellulosic materials to remove antibiotics from aqueous solution detailing the type of material, the antibiotic to be removed, experimental conditions and the removal efficiency.

Table 3. Summary of adsorption studies of organic pollutants by cellulosic materials.

Material	Antibiotic	Concentration (mg L^{-1})	Q_{max} (mg g^{-1})	pH	T (ºC)	R (%)	Ref.
Microcrystalline cellulose	AMP	--	87.7	Not adjusted	25	--	[123]
	AMX		18.5				
Carboxyalkylated cellulose nanocrystals	DOX	10-200	15.0	6.0	25	--	[124]
Cellulose Nanofibril/GO	CAP	1-100	421.2	2.0	25	78.1	[125]
	FF		418.7			76.9	
	REM		307.5			74.8	
	ETM		291.8			74.1	
	NOR		134.6			82.0	
	OFL		128.3			81.1	
	TAP		431.3			77.9	
	PNG		475.4			76.8	
	CFX		381.6			76.1	
	AMX		230.7			69.9	
	SQX		238.5			80.1	
	SDZ		228.9			80.3	
	SMR		327.8			80.0	
	SPY		227.3			79.4	
	SMZ		302.7			77.4	
	SMX		219.6			77.1	
	DOX		501.1			90.5	
	CTC		478.9			88.3	
	OTC		486.7			87.9	
	TC		454.6			82.1	
Cellulose nanocrystals /graphene oxide composite	LH	10	55.7	4.0	40	--	[126]
Carboxylated cellulose nanofiber/montmorillonite	LH	5-70	65.9	4.0	40	94.0	[127]
Laminated GO-CNC membranes	NOR	1.00	--	6.5	25	97.2	[128]
	LH		--			90.9	
Carboxymethyl cellulose acrylamide/Fe clay	CIP	10.0	57.8	5.0	35	92.0	[129]
	LH		38.0			93.0	
carboxymethyl cellulose/κ-carrageenan composites	CIP	14.7-132	421.1	5.0	25	--	[130]
Nanocellulose hydrogel	NAF	10-500	43.1	6.0	25	70	[131]
Cellulose/Ca-MMT	TC	80.0	230.5	2.0	30	--	[132]
Fe(III)-loaded cellulose nanofibers	TC	4-500	294	4.0	35	--	[133]
	CTC		233			--	
	OTC		500			--	
GO/carboxymethyl cellulose nanocomposites	OTC	200	102	5.0	30		[134]
β-Cyclodextrin/carboxymethyl cellulose Hydrogel	OTC	200	27.2	8.0	30	--	[135]
Copper-CMC nanoparticles	TC	0.50	1.11	7.5	25	90	[136]
UiO-66/ZIF-8/ polydopamine@cellulose acetate	TC	300	291	7.0	25	67	[137]
Rice Husk modified polydiallyldimethylammonium chloride onto silica	AMX	10.0	--	10	25	92.3	[121]
Olive stone LM	AMX	200	1.33×10^7	Not adjusted	25	95.0	[138]
Mg-Al layered double hydroxide/cellulose nanocomposite beads.	AMX	20-120	138	Not adjusted	45	--	[139]
Lignocellulosic substrate from wheat bran	ENR	0.72-316	94.5	6.0	20	100	[140]

LIGNIN

Lignin, one of the constituents of lignocellulosic biomass along with cellulose and hemicellulose, is a material relatively less studied and poses greater challenges for the preparation of adsorbents for antibiotics removal. Lignin is a complex aromatic macromolecule and is considered the second most abundant biomass on Earth after cellulose [141]. It has a molecular weight ranging from 1000 to 20000 g mol^{-1}, and its chemical structure is not well-defined. Regardless of the plant source and extraction process employed, lignin is primarily composed of three phenylpropane monomers: sinapyl alcohol, coniferyl alcohol, and ρ-coumaryl alcohol (see Figure 6) [142].

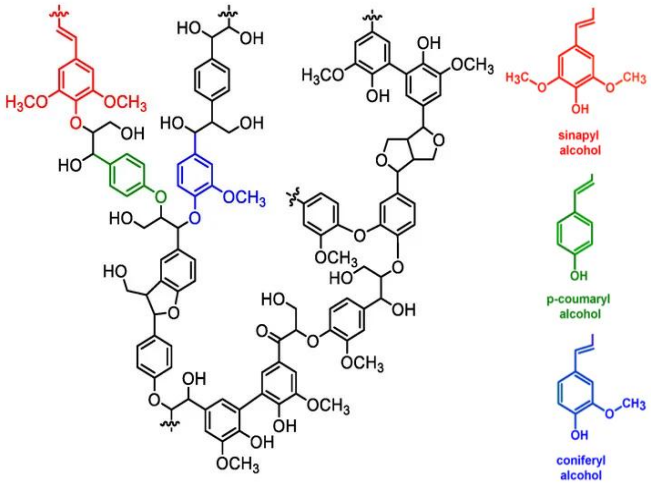

Figure 6. The lignin structure model and principal phenolic chemical structure present in lignin [142].

Lignin possesses various functional groups, including hydroxyl, carbonyl, methoxyl, and carboxyl, which can serve as adsorption sites [143]. However, due to the low uniformity of its chains, intermolecular bonds are formed, leading to a decrease in its adsorption capacity [143]. Lignin is primarily obtained as a by-product of the paper industry, and the type of lignin obtained depends on the specific process used. Alkaline lignin is obtained from the kraft process, hydrolytic lignin is derived from enzymatic hydrolysis, organosolv lignin is produced through the organo-soluble process, and lignosulfonates are obtained from the sulfite process [142]. Lignin finds applications in various industries, including the petrochemical industry, where it is used as a binding material in lithium batteries, as well as a raw material to produce new polymeric materials [144]. One recent development is the utilization of lignin in the production of hydrogels and aerogels for the removal of toxic compounds [145]. Lignin has also been employed in the preparation of hydrogels for the adsorption of organic contaminants. Its chemical structure, rich in -OH and phenolic functional groups, enables it to enhance the performance of hydrogels in removing pollutants [146]. In addition, the lignin functional groups can be chemically modified, incorporating the $-SO_3H$ and $-CONH_2$ groups previously described or combined with vinyl monomers with abundant and diverse functional groups, adding new active adsorption sites and thus improving the adsorption capacity of the material [110].

In this context, Augustine et al. investigated and characterized the effective removal of a series of drugs with different chemical characteristics using unmodified and cationized lignin nanoparticles [147]. They verified that the unmodified nanoparticles have a low surface charge, and therefore, a poor adsorption potential against pharmaceutical products with a linear structure due to the low electrostatic attraction generated. However, adsorption was more effective against aromatic pharmaceuticals, possibly because π-π interactions contribute to contaminant retention [147].

REMOVAL OF ANTIBIOTICS USING LIGNIN AND LIGNIN-BASED MATERIALS

In an insightful study, Gao et al. investigated the adsorption behavior of different lignin-based adsorbents for the removal of OFL antibiotics from water solutions. They focused on two series of lignin-based adsorbents: cross-linked lignin (LNEs) with varying crosslinking densities and carboxymethyl cross-linked lignin (LNECs) with different degrees of carboxymethyl substitution [148]. Both LNEs and LNECs exhibited excellent performance in OFL adsorption, with a maximum adsorption capacity of 300 mg g^{-1}. The content and distribution of oxygen-containing groups in these lignin-based adsorbents were strongly influenced by the crosslinking density and degree of carboxymethyl substitution, which played crucial roles in OFL adsorption. The study also revealed that the adsorption process of LNEs and LNECs was pH-dependent and involved multiple mechanisms such as hydrogen bonds, electrostatic attraction, π-π interactions, and negative charge-assisted hydrogen bonds. In a more recent investigation by Gong et al., phosphorylated alkali lignin (PAL) microparticles were fabricated through a simple one-pot method, and their adsorption behavior was studied using LH as a model antibiotic in batch mode [149]. The results demonstrated a remarkable maximum adsorption capacity of 389 mg g^{-1} for LH. Moreover, PAL showed promising applicability for the adsorption of other antibiotics such as TC and SDZ, with adsorption amounts exceeding 220 mg g^{-1} for both antibiotics. These findings highlight the great potential of PAL for antibiotic removal applications.

Continuing with lignin materials, Gao et al. fabricated a series of actinia-shaped lignin-based adsorbents (LNAEs) modified with poly(acrylic acid) (PAA) as tentacles [150]. These LNAEs were employed for the removal of OFL and CIP from water, exhibiting maximum adsorption capacities of 304 mg g^{-1} and 357 mg g^{-1} at pH 6.00, respectively. The adsorption processes were mainly attributed to electrostatic attraction and hydrogen bonding, with hydrogen bonding playing a more significant role than electrostatic attraction, as indicated by both experimental and calculation results. In another study, Chen et al. prepared a BC using sulfonated lignin and found that it exhibited a maximum adsorption capacity of 1163 mg g^{-1} for TC. Incorporating the $-SO_3H$ group significantly enhanced the formation of sulfonated bonds, leading to a substantial improvement in the adsorption performance of TC. These findings highlight the potential of lignin-based materials for the removal of antibiotics, demonstrating their diverse structures and functionalities that can be tailored for effective adsorption [151].

To combine the properties of BC and lignin materials, Xiang et al., prepared corn stalk-based (CS) and wheat straw-based (WS) BC modified with lignin and investigated their potential for TC removal from wastewater [152]. The lignin-impregnated wheat-straw BC (WS-L) exhibited a maximum adsorption capacity of 31.5 mg g^{-1}, which was 1.89 times higher compared to the corresponding raw BC. This enhancement was attributed to the development of an excellent pore structure through lignin impregnation and subsequent carbonization. On the other hand, for CS-L, the maximum adsorption capacity for TC was 21.5 mg g^{-1}. These findings highlight the successful modification of BC with lignin, resulting in improved adsorption performance for TC removal.

Table 4 details a summary of the maximum adsorption capacity of emerging contaminants by lignin-based materials from the studies described above and other reports found in the literature.

Table 4. Summary of adsorption studies of organic pollutants by lignin materials.

Material	Antibiotic	Concentration (mg L^{-1})	Q_{max} (mg g^{-1})	pH	T (°C)	R (%)	Ref.
Carboxymethyl cross-linked lignin	OFL	18-90.4	300	8.0	25	--	[128]
PAL microparticles	LH	80.0	389	7.0	45	99.9%	[149]
Actinia-shaped lignin modified with poly(acrylic acid)	OFL	72.3	304	6.0	25	--	[150]
	CIP	73.6	357	6.0	25	--	
Eucommia ulmoides Lignin-based BC	TC	10-400	1163	6.0	55	--	[151]
Lignin-impregnated wheat-straw BC	TC	1-15	31.5	7.0	25	--	[152]

OUTLOOK AND PERSPECTIVES

In this review, the use of various biomass-derived adsorbents for removing antibiotics from water solutions has been discussed. Most of these studies have been conducted at the lab-scale level and typically involve batch experiments. These lab-scale studies provide valuable insights into the adsorption capabilities and performance of the different adsorbent materials. It was also addressed that pharmaceutical pollution in sewage effluent has constantly grown as the drug usage per unit population also increases, therefore, focusing on water remediation at the pilot or industrial scale must be considered for future investigations. Adsorption has emerged as the key tool for removing antibiotic contaminants since it does not produce new products (by-products), that could be released into the environment, such as oxidation processes. Nevertheless, adsorption needs a substantial volume of adsorbent, which, after use, must be either restored for further adsorption cycles or discarded. Another issue that should be taken into account is that the recovered pharmaceuticals and/or derivatives must be discarded properly. In this context, BC has emerged as an interesting adsorbent since it can be inexpensive, especially if it is created from agricultural wastes, and by-products of biofuel production, among others. Once BC has completed its adsorption life cycle, is frequently burnt to eliminate the organic pollutants adsorbed in it. Nevertheless, industrial uses to a broad extent have yet to be developed. Another focus for future investigations should examine multicomponent adsorption, adsorption recovery, and the addition of components capable of degrading drugs into less harmful compounds in certain reaction conditions. In this context, composite materials with more than one feature could be employed as multipurpose adsorbents that can be used in a series of systems like adsorptive processes followed by catalysis -photocatalysis degradation or ozonation processes.

The further increase in the number of research publications regarding non-conventional and less-expensive feedstocks for adsorbent preparation needs intensive investigation in practical applications like fixed-bed adsorption and adsorbent regeneration that will be valuable information reflecting concrete systems and realistic measurement parameters. Additionally, a great variety of adsorbent materials has been reported in the literature, in which biopolymer-based adsorbents stand above others, due to their efficient antibiotic adsorption and that too their least ecological and environmental impact.

CONCLUSIONS

In this comprehensive review, a thorough examination of antibiotic removal from water sources has been conducted, highlighting the significant and recent scientific reports that focus on using environmentally friendly feedstocks to develop adsorptive materials. In general, it can be asserted that adsorption is among the most effective methods for removing antibiotics from polluted water, consistently demonstrating efficacies exceeding 90%. AC stands out as the most extensively studied and widely used adsorbent, exhibiting exceptional effectiveness in antibiotic removal. However, the major drawbacks associated with AC are the high material costs and potentially high regeneration costs, which hinder its large-scale implementation and utilization. On the other hand, BCs have recently emerged as better and more cost-effective materials due to their easy preparation from a broad range of feedstocks and precursors. In recent years, LM have also been considered for the removal of antibiotics, however, investigations into their adsorptive properties are still in their infancy and more studies should be carried out, due to their promising results that have been discussed in this review. Indeed, while the adsorbents summarized in this review have demonstrated efficient removal of various antibiotics, further studies on the mechanism of antibiotic adsorption are necessary to gain a deeper understanding of the interactions between the adsorbent material and the pollutants. Exploring the mechanism will aid in the development of functionalized adsorbents with improved selectivity and specificity for antibiotic removal. Several investigations have already indicated that the adsorption mechanisms may involve electrostatic interactions, hydrogen bonding, π–π interactions, hydrophobic interactions, and pore diffusion. Comprehensive knowledge of the molecular adsorption mechanisms will not only contribute to better methods for regenerating spent adsorbents but also facilitate the preparation and application of low-cost and highly effective adsorbents for removing antibiotic pollutants from sewerage and water effluents. Therefore, further research and exploration of the adsorption mechanisms are essential for advancing the field and addressing the challenges associated with antibiotic removal.

ACKNOWLEDGEMENTS

The authors thank FONDECYT [Grant number 1231498], ANID, PCI [Grant number NSFC190021].

REFERENCES

1. Bhattacharjee, M.K. Chemistry of Antibiotics and Related Drugs; Springer International Publishing: Cham, 2016; ISBN 9783319407449.
2. Stockwell, V.O.; Duffy, B. Use of Antibiotics in Plant Agriculture: -EN- -FR- Utilisation Des Antibiotiques En Agriculture (Productions Végétales) -ES- Uso de Antibióticos En La Agricultura. Rev. Sci. Tech. 2012, 31, 199–210, doi:10.20506/rst.31.1.2104.
3. Landers, T.F.; Cohen, B.; Wittum, T.E.; Larson, E.L. A Review of Antibiotic Use in Food Animals: Perspective, Policy, and Potential. Public Health Rep. 2012, 127, 4–22, doi:10.1177/003335491212700103.
4. Kucers, A.; Crowe, S.; Grayson, M.; Hoy, J. The Use of Antibiotics, 5Ed: A Clinical Review of Antibacterial, Antifungal and Antiviral Drugs; CRC Press: Boca Raton, FL, 1997; ISBN 9780750601559.
5. Machowska, A.; Stålsby Lundborg, C. Drivers of Irrational Use of Antibiotics in Europe. Int. J. Environ. Res. Public Health 2018, 16, 27, doi:10.3390/ijerph16010027.
6. Kümmerer, K. Antibiotics in the Aquatic Environment – A Review – Part II. Chemosphere 2009, 75, 435–441, doi:10.1016/j.chemosphere.2008.12.006.
7. Larsson, D.G.J. Antibiotics in the Environment. Ups. J. Med. Sci. 2014, 119, 108–112, doi:10.3109/03009734.2014.896438.
8. Kummerer, K. Significance of Antibiotics in the Environment. J. Antimicrob. Chemother. 2003, 52, 5–7, doi:10.1093/jac/dkg293.
9. Grenni, P.; Ancona, V.; Barra Caracciolo, A. Ecological Effects of Antibiotics on Natural Ecosystems: A Review. Microchem. J. 2018, 136, 25–39, doi:10.1016/j.microc.2017.02.006.
10. Gothwal, R.; Shashidhar, T. Antibiotic Pollution in the Environment: A Review. Clean (Weinh.) 2015, 43, 479–489, doi:10.1002/clen.201300989.
11. Danner, M.-C.; Robertson, A.; Behrends, V.; Reiss, J. Antibiotic Pollution in Surface Fresh Waters: Occurrence and Effects. Sci. Total Environ. 2019, 664, 793–804, doi:10.1016/j.scitotenv.2019.01.406.
12. Godoy, M.; Sánchez, J. Antibiotics as Emerging Pollutants in Water and Its Treatment. In Antibiotic Materials in Healthcare; Elsevier, 2020; pp. 221–230.
13. Sanganyado, E.; Gwenzi, W. Antibiotic Resistance in Drinking Water Systems: Occurrence, Removal, and Human Health Risks. Sci. Total Environ. 2019, 669, 785–797, doi:10.1016/j.scitotenv.2019.03.162.
14. Dutta, J.; Mala, A.A. Removal of Antibiotics from the Water Environment by the Adsorption Technologies: A Review. Water Sci. Technol. 2020, doi:10.2166/wst.2020.335.
15. Crini, G.; Lichtfouse, E.; Wilson, L.D.; Morin-Crini, N. Conventional and Non-Conventional Adsorbents for Wastewater Treatment. Environ. Chem. Lett. 2019, 17, 195–213, doi:10.1007/s10311-018-0786-8.
16. Vinayagam, V.; Murugan, S.; Kumaresan, R.; Narayanan, M.; Sillanpää, M.; Viet N Vo, D.; Kushwaha, O.S.; Jenis, P.; Potdar, P.; Gadiya, S. Sustainable Adsorbents for the Removal of Pharmaceuticals from Wastewater: A Review. Chemosphere 2022, 300, 134597, doi:10.1016/j.chemosphere.2022.134597.
17. Yaashikaa, P.R.; Kumar, P.S.; Varjani, S.; Saravanan, A. A Critical Review on the Biochar Production Techniques, Characterization, Stability and Applications for Circular Bioeconomy. Biotechnol. Rep. (Amst.) 2020, 28, e00570, doi:10.1016/j.btre.2020.e00570.
18. Krasucka, P.; Pan, B.; Sik Ok, Y.; Mohan, D.; Sarkar, B.; Oleszczuk, P. Engineered Biochar – A Sustainable Solution for the Removal of Antibiotics from Water. Chem. Eng. J. 2021, 405, 126926, doi:10.1016/j.cej.2020.126926.
19. Eniola, J.O.; Kumar, R.; Barakat, M.A. Adsorptive Removal of Antibiotics from Water over Natural and Modified Adsorbents. Environ. Sci. Pollut. Res. Int. 2019, 26, 34775–34788, doi:10.1007/s11356-019-06641-6.
20. Ahmed, M.B.; Zhou, J.L.; Ngo, H.H.; Guo, W. Adsorptive Removal of Antibiotics from Water and Wastewater: Progress and Challenges. Sci. Total Environ. 2015, 532, 112–126, doi:10.1016/j.scitotenv.2015.05.130.
21. Malakootian, M.; Yaseri, M.; Faraji, M. Removal of Antibiotics from Aqueous Solutions by Nanoparticles: A Systematic Review and Meta-Analysis. Environ. Sci. Pollut. Res. Int. 2019, 26, 8444–8458, doi:10.1007/s11356-019-04227-w.
22. Alegbeleye, O.; Daramola, O.B.; Adetunji, A.T.; Ore, O.T.; Ayantunji, Y.J.; Omole, R.K.; Ajagbe, D.; Adekoya, S.O. Efficient Removal of Antibiotics from Water Resources Is a Public Health Priority: A Critical Assessment of the Efficacy of Some Remediation Strategies for Antibiotics in Water. Environ. Sci. Pollut. Res. Int. 2022, 29, 56948–57020, doi:10.1007/s11356-022-21252-4.

23. Mangla, D.; Annu; Sharma, A.; Ikram, S. Critical Review on Adsorptive Removal of Antibiotics: Present Situation, Challenges and Future Perspective. J. Hazard. Mater. 2022, 425, 127946, doi:10.1016/j.jhazmat.2021.127946.
24. Lima, L.M.; Silva, B.N.M. da; Barbosa, G.; Barreiro, E.J. β-Lactam Antibiotics: An Overview from a Medicinal Chemistry Perspective. Eur. J. Med. Chem. 2020, 208, 112829, doi:10.1016/j.ejmech.2020.112829.
25. Becker, B.; Cooper, M.A. Aminoglycoside Antibiotics in the 21st Century. ACS Chem. Biol. 2013, 8, 105–115, doi:10.1021/cb3005116.
26. Macrolide Antibiotics; Elsevier, 2003; ISBN 9780125264518.
27. Mazzei, T.; Mini, E.; Novelli, A.; Periti, P. Chemistry and Mode of Action of Macrolides. J. Antimicrob. Chemother. 1993, 31, 1–9, doi:10.1093/jac/31.suppl_c.1.
28. Sharma, P.C.; Jain, A.; Jain, S. Fluoroquinolone Antibacterials: A Review on Chemistry, Microbiology and Therapeutic Prospects. Acta Pol. Pharm. 2009, 66.
29. Van Doorslaer, X.; Dewulf, J.; Van Langenhove, H.; Demeestere, K. Fluoroquinolone Antibiotics: An Emerging Class of Environmental Micropollutants. Sci. Total Environ. 2014, 500–501, 250–269, doi:10.1016/j.scitotenv.2014.08.075.
30. Daghrir, R.; Drogui, P. Tetracycline Antibiotics in the Environment: A Review. Environ. Chem. Lett. 2013, 11, 209–227, doi:10.1007/s10311-013-0404-8.
31. Zakeri, B.; Wright, G.D. Chemical Biology of Tetracycline AntibioticsThis Paper Is One of a Selection of Papers Published in This Special Issue, Entitled CSBMCB — Systems and Chemical Biology, and Has Undergone the Journal's Usual Peer Review Process. Biochem. Cell Biol. 2008, 86, 124–136, doi:10.1139/o08-002.
32. Vass, M.; Hruska, K.; Franek, M. Nitrofuran Antibiotics: A Review on the Application, Prohibition and Residual Analysis. Vet. Med. (Praha) 2008, 53, 469–500, doi:10.17221/1979-vetmed.
33. Miura, K.; Reckendorf, H.K. 6 The Nitrofurans. In Progress in Medicinal Chemistry; Elsevier, 1967; pp. 320–381 ISBN 9780444533241.
34. I. H. El-Qaliei, M.; El-Gaby, M.; A. Ammar, Y.; M. ali, A.; F. Hussein, M.; A. Faraghally, F. Sulfonamides: Synthesis and the Recent Applications in Medicinal Chemistry. Egypt. J. Chem. 2020, 0, 0–0, doi:10.21608/ejchem.2020.33860.2707.
35. Chinthakindi, P.K.; Naicker, T.; Thota, N.; Govender, T.; Kruger, H.G.; Arvidsson, P.I. Sulfonimidamides in Medicinal and Agricultural Chemistry. Angew. Chem. Int. Ed Engl. 2017, 56, 4100–4109, doi:10.1002/anie.201610456.
36. Sukul, P.; Spiteller, M. Sulfonamides in the Environment as Veterinary Drugs. In Reviews of Environmental Contamination and Toxicology; Springer New York: New York, NY, 2006; pp. 67–101 ISBN 9781461270768.
37. Shah, S.S.A.; Rivera, G.; Ashfaq, M. Recent Advances in Medicinal Chemistry of Sulfonamides. Rational Design as Anti-Tumoral, Anti-Bacterial and Anti-Inflammatory Agents. Mini-Reviews in Medicinal Chemistry 13, 70–86, doi:10.2174/13895575130107.
38. Sharma, G.; Sharma, S.; Kumar, A.; Lai, C.W.; Naushad, M.; Shehnaz; Iqbal, J.; Stadler, F.J. Activated Carbon as Superadsorbent and Sustainable Material for Diverse Applications. Adsorp. Sci. Technol. 2022, 2022, 1–21, doi:10.1155/2022/4184809.
39. Ahmad, M.; Rajapaksha, A.U.; Lim, J.E.; Zhang, M.; Bolan, N.; Mohan, D.; Vithanage, M.; Lee, S.S.; Ok, Y.S. Biochar as a Sorbent for Contaminant Management in Soil and Water: A Review. Chemosphere 2014, 99, 19–33, doi:10.1016/j.chemosphere.2013.10.071.
40. Joseph, S.; Cowie, A.L.; Van Zwieten, L.; Bolan, N.; Budai, A.; Buss, W.; Cayuela, M.L.; Graber, E.R.; Ippolito, J.A.; Kuzyakov, Y.; et al. How Biochar Works, and When It Doesn't: A Review of Mechanisms Controlling Soil and Plant Responses to Biochar. Glob. Change Biol. Bioenergy 2021, 13, 1731–1764, doi:10.1111/gcbb.12885.
41. Shukla, P.; Giri, B.S.; Mishra, R.K.; Pandey, A.; Chaturvedi, P. Lignocellulosic Biomass-Based Engineered Biochar Composites: A Facile Strategy for Abatement of Emerging Pollutants and Utilization in Industrial Applications. Renew. Sustain. Energy Rev. 2021, 152, 111643, doi:10.1016/j.rser.2021.111643.
42. Salfate, G.; Sánchez, J. Rare Earth Elements Uptake by Synthetic Polymeric and Cellulose-Based Materials: A Review. Polymers (Basel) 2022, 14, 4786, doi:10.3390/polym14214786.
43. Ghiorghita, C.-A.; Dinu, M.V.; Lazar, M.M.; Dragan, E.S. Polysaccharide-Based Composite Hydrogels as Sustainable Materials for Removal of Pollutants from Wastewater. Molecules 2022, 27, 8574, doi:10.3390/molecules27238574.
44. Tran, H.N.; You, S.-J.; Hosseini-Bandegharaei, A.; Chao, H.-P. Mistakes and Inconsistencies Regarding Adsorption of Contaminants from Aqueous Solutions: A Critical Review. Water Res. 2017, 120, 88–116, doi:10.1016/j.watres.2017.04.014.
45. Battak, N.; Kamin, Z.; Bahrun, M.H.V.; Chiam, C.K.; Peter, E.; Bono, A. Removal of Trace Plant Antibiotics from Water Systems by Adsorption: A Review. J. Mol. Liq. 2022, 45, 1721–1730, doi:10.1002/ceat.202200032.
46. Kumar, K.V.; Porkodi, K. Relation between Some Two- and Three-Parameter Isotherm Models for the Sorption of Methylene Blue onto Lemon Peel. J. Hazard. Mater. 2006, 138, 633–635, doi:10.1016/j.jhazmat.2006.06.078.
47. Rajabi, M.; Keihankhadiv, S.; Suhas; Tyagi, I.; Karri, R.R.; Chaudhary, M.; Mubarak, N.M.; Chaudhary, S.; Kumar, P.; Singh, P. Comparison and Interpretation of Isotherm Models for the Adsorption of Dyes, Proteins, Antibiotics, Pesticides and Heavy Metal Ions on Different Nanomaterials and Non-Nano Materials—a Comprehensive Review. J. Nanostructure Chem. 2023, 13, 43–65, doi:10.1007/s40097-022-00509-x.
48. Zhao, H.; Wang, Z.; Liang, Y.; Wu, T.; Chen, Y.; Yan, J.; Zhu, Y.; Ding, D. Adsorptive Decontamination of Antibiotics from Livestock Wastewater by Using Alkaline-Modified Biochar. Environ. Res. 2023, 226, 115676, doi:10.1016/j.envres.2023.115676.
49. Boulett, A.; Roa, K.; Oyarce, E.; Xiao, L.-P.; Sun, R.-C.; Pizarro, G. del C.; Sánchez, J. Reusable Hydrogels Based on Lignosulfonate and Cationic Polymer for the Removal of Cr(VI) from Wastewater. Colloids Surf. A Physicochem. Eng. Asp. 2023, 656, 130359, doi:10.1016/j.colsurfa.2022.130359.
50. Oyarce, E.; Cantero-López, P.; Roa, K.; Boulett, A.; Yáñez, O.; Santander, P.; del C. Pizarro, G.; Sánchez, J. Removal of Highly Concentrated Methylene Blue Dye by Cellulose Nanofiber Biocomposites. Int. J. Biol. Macromol. 2023, 238, 124045, doi:10.1016/j.ijbiomac.2023.124045.
51. Benjelloun, M.; Miyah, Y.; Akdemir Evrendilek, G.; Zerrouq, F.; Lairini, S. Recent Advances in Adsorption Kinetic Models: Their Application to Dye Types. Arab. J. Chem. 2021, 14, 103031, doi:10.1016/j.arabjc.2021.103031.
52. Miao, J.; Wang, F.; Chen, Y.; Zhu, Y.; Zhou, Y.; Zhang, S. The Adsorption Performance of Tetracyclines on Magnetic Graphene Oxide: A Novel Antibiotics Absorbent. J. Environ. Sci. (China) 2019, 475, 549–558, doi:10.1016/j.apsusc.2019.01.036.
53. Rostamian, R.; Behnejad, H. A Comprehensive Adsorption Study and Modeling of Antibiotics as a Pharmaceutical Waste by Graphene Oxide Nanosheets. J. Hazard. Mater. 2018, 147, 117–123, doi:10.1016/j.ecoenv.2017.08.019.
54. Yu, F.; Li, Y.; Huang, G.; Yang, C.; Chen, C.; Zhou, T.; Zhao, Y.; Ma, J. Adsorption Behavior of the Antibiotic Levofloxacin on Microplastics in the Presence of Different Heavy Metals in an Aqueous Solution. Biomass Convers. Biorefin. 2020, 260, doi:10.1016/j.chemosphere.2020.127650.
55. Azhar, M.R.; Abid, H.R.; Sun, H.; Periasamy, V.; Tadé, M.O.; Wang, S. Excellent Performance of Copper Based Metal Organic Framework in Adsorptive Removal of Toxic Sulfonamide Antibiotics from Wastewater. Ecotoxicol. Environ. Saf. 2016, 478, 344–352, doi:10.1016/j.jcis.2016.06.032.
56. Du, C.; Zhang, Z.; Yu, G.; Wu, H.; Chen, H.; Zhou, L.; Zhang, Y.; Su, Y.; Tan, S.; Yang, L.; et al. A Review of Metal Organic Framework (MOFs)-Based Materials for Antibiotics Removal via Adsorption and Photocatalysis. Water Sci. Technol. 2021, 272, 1484–1494, doi:10.1016/j.chemosphere.2020.129501.
57. Jayawardena, R.; Eldridge, D.S.; Malherbe, F. Sonochemical Synthesis of Improved Graphene Oxide for Enhanced Adsorption of Methylene Blue. Colloids Surf. A Physicochem. Eng. Asp. 2022, 650, 129587, doi:10.1016/j.colsurfa.2022.129587.
58. Tran, T.H.; Le, A.H.; Pham, T.H.; Nguyen, D.T.; Chang, S.W.; Chung, W.J.; Nguyen, D.D. Adsorption Isotherms and Kinetic Modeling of Methylene Blue Dye onto a Carbonaceous Hydrochar Adsorbent Derived from Coffee Husk Waste. Sci. Total Environ. 2020, 725, 138325, doi:10.1016/j.scitotenv.2020.138325.
59. Tran, H.N.; You, S.-J.; Chao, H.-P. Thermodynamic Parameters of Cadmium Adsorption onto Orange Peel Calculated from Various Methods: A Comparison Study. J. Environ. Chem. Eng. 2016, 4, 2671–2682, doi:10.1016/j.jece.2016.05.009.
60. Liu, Y. Is the Free Energy Change of Adsorption Correctly Calculated? J. Chem. Eng. Data 2009, 54, 1981–1985, doi:10.1021/je800661q.
61. Huang, F.-C.; Lee, C.-K.; Han, Y.-L.; Chao, W.-C.; Chao, H.-P. Preparation of Activated Carbon Using Micro-Nano Carbon Spheres through Chemical Activation. J. Taiwan Inst. Chem. Eng. 2014, 45, 2805–2812, doi:10.1016/j.jtice.2014.08.004.

62. Sawant, S.Y.; Munusamy, K.; Somani, R.S.; John, M.; Newalkar, B.L.; Bajaj, H.C. Precursor Suitability and Pilot Scale Production of Super Activated Carbon for Greenhouse Gas Adsorption and Fuel Gas Storage. Chem. Eng. J. 2017, 315, 415–425, doi:10.1016/j.cej.2017.01.037.
63. Heidarinejad, Z.; Dehghani, M.H.; Heidari, M.; Javedan, G.; Ali, I.; Sillanpää, M. Methods for Preparation and Activation of Activated Carbon: A Review. Environ. Chem. Lett. 2020, 18, 393–415, doi:10.1007/s10311-019-00955-0.
64. Yu, F.; Li, Y.; Han, S.; Ma, J. Adsorptive Removal of Antibiotics from Aqueous Solution Using Carbon Materials. Chemosphere 2016, 153, 365–385, doi:10.1016/j.chemosphere.2016.03.083.
65. Pallarés, J.; González-Cencerrado, A.; Arauzo, I. Production and Characterization of Activated Carbon from Barley Straw by Physical Activation with Carbon Dioxide and Steam. Biomass Bioenergy 2018, 115, 64–73, doi:10.1016/j.biombioe.2018.04.015.
66. Gratuito, M.K.B.; Panyathanmaporn, T.; Chumnanklang, R.-A.; Sirinuntawittaya, N.; Dutta, A. Production of Activated Carbon from Coconut Shell: Optimization Using Response Surface Methodology. Bioresour. Technol. 2008, 99, 4887–4895, doi:10.1016/j.biortech.2007.09.042.
67. Rambabu, N.; Rao, B.V.S.K.; Surisetty, V.R.; Das, U.; Dalai, A.K. Production, Characterization, and Evaluation of Activated Carbons from de-Oiled Canola Meal for Environmental Applications. Ind. Crops Prod. 2015, 65, 572–581, doi:10.1016/j.indcrop.2014.09.046.
68. El-Shafey, E.-S.I.; Al-Lawati, H.; Al-Sumri, A.S. Ciprofloxacin Adsorption from Aqueous Solution onto Chemically Prepared Carbon from Date Palm Leaflets. J. Environ. Sci. (China) 2012, 24, 1579–1586, doi:10.1016/s1001-0742(11)60949-2.
69. Chandrasekaran, A.; Patra, C.; Narayanasamy, S.; Subbiah, S. Adsorptive Removal of Ciprofloxacin and Amoxicillin from Single and Binary Aqueous Systems Using Acid-Activated Carbon from Prosopis Juliflora. Environ. Res. 2020, 188, 109825, doi:10.1016/j.envres.2020.109825.
70. Huang, L.; Wang, M.; Shi, C.; Huang, J.; Zhang, B. Adsorption of Tetracycline and Ciprofloxacin on Activated Carbon Prepared from Lignin with H3PO4Activation. Desalination Water Treat. 2014, 52, 2678–2687, doi:10.1080/19443994.2013.833873.
71. Agboola, O.S.; Bello, O.S. Enhanced Adsorption of Ciprofloxacin from Aqueous Solutions Using Functionalized Banana Stalk. Biomass Convers. Biorefin. 2022, 12, 5463–5478, doi:10.1007/s13399-020-01038-9.
72. Guellati, A.; Maachi, R.; Chaabane, T.; Darchen, A.; Danish, M. Aluminum Dispersed Bamboo Activated Carbon Production for Effective Removal of Ciprofloxacin Hydrochloride Antibiotics: Optimization and Mechanism Study. J. Environ. Manage. 2022, 301, 113765, doi:10.1016/j.jenvman.2021.113765.
73. Alacabey, İ. Antibiotic Removal from the Aquatic Environment with Activated Carbon Produced from Pumpkin Seeds. Molecules 2022, 27, 1380, doi:10.3390/molecules27041380.
74. Sousa, É.M.L.; Otero, M.; Rocha, L.S.; Gil, M.V.; Ferreira, P.; Esteves, V.I.; Calisto, V. Multivariable Optimization of Activated Carbon Production from Microwave Pyrolysis of Brewery Wastes - Application in the Removal of Antibiotics from Water. J. Hazard. Mater. 2022, 431, 128556, doi:10.1016/j.jhazmat.2022.128556.
75. Darweesh, T.M.; Ahmed, M.J. Adsorption of Ciprofloxacin and Norfloxacin from Aqueous Solution onto Granular Activated Carbon in Fixed Bed Column. Ecotoxicol. Environ. Saf. 2017, 138, 139–145, doi:10.1016/j.ecoenv.2016.12.032.
76. Bednárek, J.; Matějová, L.; Koutník, I.; Vráblová, M.; Cruz, G.J.F.; Strašák, T.; Šiler, P.; Hrbáč, J. Revelation of High-Adsorption-Performance Activated Carbon for Removal of Fluoroquinolone Antibiotics from Water. Biomass Convers. Biorefin. 2022, doi:10.1007/s13399-022-02577-z.
77. Liu, H.; Ning, W.; Cheng, P.; Zhang, J.; Wang, Y.; Zhang, C. Evaluation of Animal Hairs-Based Activated Carbon for Sorption of Norfloxacin and Acetaminophen by Comparing with Cattail Fiber-Based Activated Carbon. J. Anal. Appl. Pyrolysis 2013, 101, 156–165, doi:10.1016/j.jaap.2013.01.016.
78. Palacio, D.A.; Urbano, B.F.; Rivas, B.L. Application of Nanocomposite Polyelectrolytes for the Removal of Antibiotics as Emerging Pollutants in Water. J. Water Proc.engineering 2022, 46, 102582, doi:10.1016/j.jwpe.2022.102582.
79. Moreira, N.F.F.; Orge, C.A.; Ribeiro, A.R.; Faria, J.L.; Nunes, O.C.; Pereira, M.F.R.; Silva, A.M.T. Fast Mineralization and Detoxification of Amoxicillin and Diclofenac by Photocatalytic Ozonation and Application to an Urban Wastewater. Water Res. 2015, 87, 87–96, doi:10.1016/j.watres.2015.08.059.
80. Balarak, D.; Mostafapour, F.; Akbari, H.; Joghtaei, A. Adsorption of Amoxicillin Antibiotic from Pharmaceutical Wastewater by Activated Carbon Prepared from Azolla Filiculoides. J. Pharm. Res. Int. 2017, 18, 1–13, doi:10.9734/jpri/2017/35607.
81. Berges, J.; Moles, S.; Ormad, M.P.; Mosteo, R.; Gómez, J. Antibiotics Removal from Aquatic Environments: Adsorption of Enrofloxacin, Trimethoprim, Sulfadiazine, and Amoxicillin on Vegetal Powdered Activated Carbon. Environ. Sci. Pollut. Res. Int. 2021, 28, 8442–8452, doi:10.1007/s11356-020-10972-0.
82. Hashemzadeh, F.; Ariannezhad, M.; Derakhshandeh, S.H. Evaluation of Cephalexin and Amoxicillin Removal from Aqueous Media Using Activated Carbon Produced from Aloe Vera Leaf Waste. Chem. Phys. Lett. 2022, 800, 139656, doi:10.1016/j.cplett.2022.139656.
83. Ali, I.; Afshinb, S.; Poureshgh, Y.; Azari, A.; Rashtbari, Y.; Feizizadeh, A.; Hamzezadeh, A.; Fazlzadeh, M. Green Preparation of Activated Carbon from Pomegranate Peel Coated with Zero-Valent Iron Nanoparticles (NZVI) and Isotherm and Kinetic Studies of Amoxicillin Removal in Water. Environ. Sci. Pollut. Res. Int. 2020, 27, 36732–36743, doi:10.1007/s11356-020-09310-1.
84. Ovung, A.; Bhattacharyya, J. Sulfonamide Drugs: Structure, Antibacterial Property, Toxicity, and Biophysical Interactions. Biophys. Rev. 2021, 13, 259–272, doi:10.1007/s12551-021-00795-9.
85. Fan, Y.; Zheng, C.; Hou, H. Preparation of Granular Activated Carbon and Its Mechanism in the Removal of Isoniazid, Sulfamethoxazole, Thiamphenicol, and Doxycycline from Aqueous Solution. Environ. Eng. Sci. 2019, 36, 1027–1040, doi:10.1089/ees.2018.0472.
86. Jaria, G.; Calisto, V.; Gil, M.V.; Ferreira, P.; Santos, S.M.; Otero, M.; Esteves, V.I. Effects of Thiol Functionalization of a Waste-Derived Activated Carbon on the Adsorption of Sulfamethoxazole from Water: Kinetic, Equilibrium and Thermodynamic Studies. J. Mol. Liq. 2021, 323, 115003, doi:10.1016/j.molliq.2020.115003.
87. Hu, W.; Niu, Y.; Dong, K.; Wang, D. Removal of Sulfamethoxazole from Aqueous Solution onto Bagasse-Derived Activated Carbon: Response Surface Methodology, Isotherm and Kinetics Studies. J. Mol. Liq. 2022, 347, 118141, doi:10.1016/j.molliq.2021.118141.
88. Akhtar, J.; Amin, N.S.; Aris, A. Combined Adsorption and Catalytic Ozonation for Removal of Sulfamethoxazole Using Fe2O3/CeO2 Loaded Activated Carbon. Chem. Eng. J. 2011, 170, 136–144, doi:10.1016/j.cej.2011.03.043.
89. Teixeira, S.; Delerue-Matos, C.; Santos, L. Application of Experimental Design Methodology to Optimize Antibiotics Removal by Walnut Shell Based Activated Carbon. Sci. Total Environ. 2019, 646, 168–176, doi:10.1016/j.scitotenv.2018.07.204.
90. Askari, R.; Afshin, S.; Rashtbari, Y.; Moharrami, A.; Mohammadi, F.; Vosuoghi, M.; Dargahi, A. Synthesis of Activated Carbon from Walnut Wood and Magnetized with Cobalt Ferrite (CoFe2O4) and Its Application in Removal of Cephalexin from Aqueous Solutions. J. Dispers. Sci. Technol. 2023, 44, 1183–1194, doi:10.1080/01932691.2021.2008421.
91. Ahmed, M.J.; Theydan, S.K. Adsorption of Cephalexin onto Activated Carbons from Albizia Lebbeck Seed Pods by Microwave-Induced KOH and K2CO3 Activations. Chem. Eng. J. 2012, 211–212, 200–207, doi:10.1016/j.cej.2012.09.089.
92. Pouretedal, H.R.; Sadegh, N. Effective Removal of Amoxicillin, Cephalexin, Tetracycline and Penicillin G from Aqueous Solutions Using Activated Carbon Nanoparticles Prepared from Vine Wood. J. Water Proc.engineering 2014, 1, 64–73, doi:10.1016/j.jwpe.2014.03.006.
93. Chamberlain, R.E. Chemotherapeutic Properties of Prominent Nitrofurans. J. Antimicrob. Chemother. 1976, 2, 325–336, doi:10.1093/jac/2.4.325.
94. Ahmed, M.J.; Theydan, S.K. Microwave Assisted Preparation of Microporous Activated Carbon from Siris Seed Pods for Adsorption of Metronidazole Antibiotic. Chem. Eng. J. 2013, 214, 310–318, doi:10.1016/j.cej.2012.10.101.
95. Ebili, P.E.; Auta, M.; Obayomi, K.S.; Okafor, J.O.; Yahya, M.D.; Faruq, A.A. Comparative Analysis of Linear and Nonlinear Equilibrium Models for the Removal of Metronidazole by Tea Waste Activated Carbon. Water Sci. Technol. 2020, 82, 1484–1494, doi:10.2166/wst.2020.428.
96. Manjunath, S.V.; Kumar, M. Simultaneous Removal of Antibiotic and Nutrients via Prosopis Juliflora Activated Carbon Column: Performance Evaluation, Effect of Operational Parameters and Breakthrough Modeling. Chemosphere 2021, 262, 127820, doi:10.1016/j.chemosphere.2020.127820.
97. Wang, W.; Kang, R.; Yin, Y.; Tu, S.; Ye, L. Two-Step Pyrolysis Biochar Derived from Agro-Waste for Antibiotics Removal: Mechanisms and Stability. Chemosphere 2022, 292, 133454, doi:10.1016/j.chemosphere.2021.133454.
98. Sun, Y.; Gao, B.; Yao, Y.; Fang, J.; Zhang, M.; Zhou, Y.; Chen, H.; Yang, L. Effects of Feedstock Type, Production Method, and Pyrolysis Temperature on Biochar and Hydrochar Properties. Chem. Eng. J. 2014, 240, 574–578, doi:10.1016/j.cej.2013.10.081.

99. Li, J.; Yu, G.; Pan, L.; Li, C.; You, F.; Xie, S.; Wang, Y.; Ma, J.; Shang, X. Study of Ciprofloxacin Removal by Biochar Obtained from Used Tea Leaves. J. Environ. Sci. (China) 2018, 73, 20–30, doi:10.1016/j.jes.2017.12.024.
100. Zeng, Z.-W.; Tian, S.-R.; Liu, Y.-G.; Tan, X.-F.; Zeng, G.-M.; Jiang, L.-H.; Yin, Z.-H.; Liu, N.; Liu, S.-B.; Li, J. Comparative Study of Rice Husk Biochars for Aqueous Antibiotics Removal. J. Chem. Technol. Biotechnol. 2018, 93, 1075–1084, doi:10.1002/jctb.5464.
101. Li, J.; Yu, G.; Pan, L.; Li, C.; You, F.; Wang, Y. Ciprofloxacin Adsorption by Biochar Derived from Co-Pyrolysis of Sewage Sludge and Bamboo Waste. Environ. Sci. Pollut. Res. Int. 2020, 27, 22806–22817, doi:10.1007/s11356-020-08333-y.
102. Patel, M.; Kumar, R.; Pittman, C.U., Jr; Mohan, D. Ciprofloxacin and Acetaminophen Sorption onto Banana Peel Biochars: Environmental and Process Parameter Influences. Environ. Res. 2021, 201, 111218, doi:10.1016/j.envres.2021.111218.
103. Zhang, X.; Chu, Y.; Zhang, H.; Hu, J.; Wu, F.; Wu, X.; Shen, G.; Yang, Y.; Wang, B.; Wang, X. A Mechanistic Study on Removal Efficiency of Four Antibiotics by Animal and Plant Origin Precursors-Derived Biochars. Sci. Total Environ. 2021, 772, 145468, doi:10.1016/j.scitotenv.2021.145468.
104. Hu, Y.; Zhu, Y.; Zhang, Y.; Lin, T.; Zeng, G.; Zhang, S.; Wang, Y.; He, W.; Zhang, M.; Long, H. An Efficient Adsorbent: Simultaneous Activated and Magnetic ZnO Doped Biochar Derived from Camphor Leaves for Ciprofloxacin Adsorption. Bioresour. Technol. 2019, 288, 121511, doi:10.1016/j.biortech.2019.121511.
105. Zhou, Y.; Cao, S.; Xi, C.; Li, X.; Zhang, L.; Wang, G.; Chen, Z. A Novel Fe3O4/Graphene Oxide/Citrus Peel-Derived Bio-Char Based Nanocomposite with Enhanced Adsorption Affinity and Sensitivity of Ciprofloxacin and Sparfloxacin. Bioresour. Technol. 2019, 292, 121951, doi:10.1016/j.biortech.2019.121951.
106. Sayin, F.; Akar, S.T.; Akar, T. From Green Biowaste to Water Treatment Applications: Utilization of Modified New Biochar for the Efficient Removal of Ciprofloxacin. Sustain. Chem. Pharm. 2021, 24, 100522, doi:10.1016/j.scp.2021.100522.
107. Li, R.; Wang, Z.; Guo, J.; Li, Y.; Zhang, H.; Zhu, J.; Xie, X. Enhanced Adsorption of Ciprofloxacin by KOH Modified Biochar Derived from Potato Stems and Leaves. Water Sci. Technol. 2018, 77, 1127–1136, doi:10.2166/wst.2017.636.
108. Egbedina, A.O.; Adebowale, K.O.; Olu-Owolabi, B.I.; Unuabonah, E.I.; Adesina, M.O. Green Synthesis of ZnO Coated Hybrid Biochar for the Synchronous Removal of Ciprofloxacin and Tetracycline in Wastewater. RSC Adv. 2021, 11, 18483–18492, doi:10.1039/d1ra01130h.
109. Hamadeen, H.M.; Elkhatib, E.A. New Nanostructured Activated Biochar for Effective Removal of Antibiotic Ciprofloxacin from Wastewater: Adsorption Dynamics and Mechanisms. Environ. Res. 2022, 210, 112929, doi:10.1016/j.envres.2022.112929.
110. Atugoda, T.; Gunawardane, C.; Ahmad, M.; Vithanage, M. Mechanistic Interaction of Ciprofloxacin on Zeolite Modified Seaweed (Sargassum Crassifolium) Derived Biochar: Kinetics, Isotherm and Thermodynamics. Chemosphere 2021, 281, 130676, doi:10.1016/j.chemosphere.2021.130676.
111. Nguyen, T.-B.; Truong, Q.-M.; Chen, C.-W.; Doong, R.-A.; Chen, W.-H.; Dong, C.-D. Mesoporous and Adsorption Behavior of Algal Biochar Prepared via Sequential Hydrothermal Carbonization and ZnCl2 Activation. Bioresour. Technol. 2022, 346, 126351, doi:10.1016/j.biortech.2021.126351.
112. Wu, J.; Wang, T.; Liu, Y.; Tang, W.; Geng, S.; Chen, J. Norfloxacin Adsorption and Subsequent Degradation on Ball-Milling Tailored N-Doped Biochar. Chemosphere 2022, 303, 135264, doi:10.1016/j.chemosphere.2022.135264.
113. Wan, J.; Liu, L.; Ayub, K.S.; Zhang, W.; Shen, G.; Hu, S.; Qian, X. Characterization and Adsorption Performance of Biochars Derived from Three Key Biomass Constituents. Fuel (Lond.) 2020, 269, 117142, doi:10.1016/j.fuel.2020.117142.
114. Meng, Q.; Zhang, Y.; Meng, D.; Liu, X.; Zhang, Z.; Gao, P.; Lin, A.; Hou, L. Removal of Sulfadiazine from Aqueous Solution by In-Situ Activated Biochar Derived from Cotton Shell. Environ. Res. 2020, 191, 110104, doi:10.1016/j.envres.2020.110104.
115. Sun, Y.; Zheng, L.; Zheng, X.; Xiao, D.; Yang, Y.; Zhang, Z.; Ai, B.; Sheng, Z. Adsorption of Sulfonamides in Aqueous Solution on Reusable Coconut-Shell Biochar Modified by Alkaline Activation and Magnetization. Front. Chem. 2022, 9, doi:10.3389/fchem.2021.814647.
116. Liu, S.; Wang, Y.; Feng, Z.; Wang, Y.; Sun, T. Hierarchical Porous Biochar with Ultra-High Specific Surface Area for Rapid Removal of Antibiotics from Water. New J Chem 2021, 45, 17418–17427, doi:10.1039/d1nj02686k.
117. Li, Y.; Shang, H.; Cao, Y.; Yang, C.; Feng, Y.; Yu, Y. High Performance Removal of Sulfamethoxazole Using Large Specific Area of Biochar Derived from Corncob Xylose Residue. Biochar 2022, 4, doi:10.1007/s42773-021-00128-9.
118. Chu, Z.; Zheng, B.; Wang, W.; Li, Y.; Yang, Y.; Yang, Z. Magnetic Nitrogen–Doped Biochar for Adsorptive and Oxidative Removal of Antibiotics in Aqueous Solutions. Sep. Purif. Technol. 2022, 297, 121508, doi:10.1016/j.seppur.2022.121508.
119. Thakur, V.K.; Thakur, M.K. Recent Advances in Green Hydrogels from Lignin: A Review. Int. J. Biol. Macromol. 2015, 72, 834–847, doi:10.1016/j.ijbiomac.2014.09.044.
120. Roa, K.; Oyarce, E.; Boulett, A.; ALSamman, M.; Oyarzún, D.; Pizarro, G.D.C.; Sánchez, J. Lignocellulose-Based Materials and Their Application in the Removal of Dyes from Water: A Review. Sustain. Mater. Technol. 2021, 29, e00320, doi:10.1016/j.susmat.2021.e00320.
121. Pham, T.; Bui, T.; Nguyen, V.; Bui, T.; Tran, T.; Phan, Q.; Pham, T.; Hoang, T. Adsorption of Polyelectrolyte onto Nanosilica Synthesized from Rice Husk: Characteristics, Mechanisms, and Application for Antibiotic Removal. Polymers (Basel) 2018, 10, 220, doi:10.3390/polym10020220.
122. Ventura-Cruz, S.; Tecante, A. Nanocellulose and Microcrystalline Cellulose from Agricultural Waste: Review on Isolation and Application as Reinforcement in Polymeric Matrices. Food Hydrocoll. 2021, 118, 106771, doi:10.1016/j.foodhyd.2021.106771.
123. El-Samaligy, M.S.; El-Mahrouk, G.M.; El-Kirsh, T.A. Adsorption—Desorption Effect of Microcrystalline Cellulose on Ampicillin and Amoxycillin. Int. J. Pharm. 1986, 31, 137–144, doi:10.1016/0378-5173(86)90223-1.
124. Feizi, Z.H.; Fatehi, P. Interaction of Carboxyalkylated Cellulose Nanocrystals and Antibiotics. ACS Appl. Bio Mater. 2021, 4, 4165–4175, doi:10.1021/acsabm.0c01664.
125. Yao, Q.; Fan, B.; Xiong, Y.; Jin, C.; Sun, Q.; Sheng, C. 3D Assembly Based on 2D Structure of Cellulose Nanofibril/Graphene Oxide Hybrid Aerogel for Adsorptive Removal of Antibiotics in Water. Sci. Rep. 2017, 7, doi:10.1038/srep45914.
126. Tao, J.; Yang, J.; Ma, C.; Li, J.; Du, K.; Wei, Z.; Chen, C.; Wang, Z.; Zhao, C.; Deng, X. Cellulose Nanocrystals/Graphene Oxide Composite for the Adsorption and Removal of Levofloxacin Hydrochloride Antibiotic from Aqueous Solution. R. Soc. Open Sci. 2020, 7, 200857, doi:10.1098/rsos.200857.
127. Li, J.; Tao, J.; Ma, C.; Yang, J.; Gu, T.; Liu, J. Carboxylated Cellulose Nanofiber/Montmorillonite Nanocomposite for the Removal of Levofloxacin Hydrochloride Antibiotic from Aqueous Solutions. RSC Adv. 2020, 10, 42038–42053, doi:10.1039/d0ra08987g.
128. Gao, H.; Wang, Y.; Afolabi, M.A.; Xiao, D.; Chen, Y. Incorporation of Cellulose Nanocrystals into Graphene Oxide Membranes for Efficient Antibiotic Removal at High Nutrient Recovery. ACS Appl. Mater. Interfaces 2021, 13, 14102–14111, doi:10.1021/acsami.0c20652.
129. Gopal, G.; Natarajan, C.; Mukherjee, A. Adsorptive Removal of Fluoroquinolone Antibiotics Using Green Synthesized and Highly Efficient Fe Clay Cellulose-Acrylamide Beads. Environ. Technol. Innov. 2022, 28, 102783, doi:10.1016/j.eti.2022.102783.
130. Li, N.; Gao, B.; Yang, R.; Yang, H. Simple Fabrication of Carboxymethyl Cellulose and κ-Carrageenan Composite Aerogel with Efficient Performance in Removal of Fluoroquinolone Antibiotics from Water. Front. Environ. Sci. Eng. 2022, 16, doi:10.1007/s11783-022-1568-x.
131. Cantero-López, P.; Godoy, M.; Oyarce, E.; Pizarro, G.D.C.; Xu, C.; Willför, S.; Yañez, O.; Sánchez, J. Removal of Nafcillin Sodium Monohydrate from Aqueous Solution by Hydrogels Containing Nanocellulose: An Experimental and Theoretical Study. J. Mol. Liq. 2022, 347, 117946, doi:10.1016/j.molliq.2021.117946.
132. Hu, Y.; Chen, C.; Yang, L.; Cui, J.; Hao, Q.; Sun, D. Handy Purifier Based on Bacterial Cellulose and Ca-Montmorillonite Composites for Efficient Removal of Dyes and Antibiotics. Carbohydr. Polym. 2019, 222, 115017, doi:10.1016/j.carbpol.2019.115017.
133. Lu, L.; Liu, M.; Chen, Y.; Luo, Y. Effective Removal of Tetracycline Antibiotics from Wastewater Using Practically Applicable Iron(III)-Loaded Cellulose Nanofibres. R. Soc. Open Sci. 2021, 8, 210336, doi:10.1098/rsos.210336.
134. Juengchareonpoon, K.; Wanichpongpan, P.; Boonamnuayvitaya, V. Graphene Oxide and Carboxymethylcellulose Film Modified by Citric Acid for Antibiotic Removal. J. Environ. Chem. Eng. 2021, 9, 104637, doi:10.1016/j.jece.2020.104637.
135. Juengchareonpoon, K.; Boonamnuayvitaya, V.; Wanichpongpan, P. Kinetics and Isotherms of Oxytetracycline Adsorption on B-cyclodextrin/Carboxymethylcellulose Hydrogel Films. Aquac. Res. 2019, 50, 3412–3419, doi:10.1111/are.14299.

136. ALOthman, Z.A.; Badjah, A.Y.; Alharbi, O.M.L.; Ali, I. Copper Carboxymethyl Cellulose Nanoparticles for Efficient Removal of Tetracycline Antibiotics in Water. Environ. Sci. Pollut. Res. Int. 2020, 27, 42960–42968, doi:10.1007/s11356-020-10189-1.
137. Abd El-Monaem, E.M.; Omer, A.M.; Khalifa, R.E.; Eltaweil, A.S. Floatable Cellulose Acetate Beads Embedded with Flower-like Zwitterionic Binary MOF/PDA for Efficient Removal of Tetracycline. J. Colloid Interface Sci. 2022, 620, 333–345, doi:10.1016/j.jcis.2022.04.010.
138. Saldarriaga, J.F.; Montoya, N.A.; Estiati, I.; Aguayo, A.T.; Aguado, R.; Olazar, M. Unburned Material from Biomass Combustion as Low-Cost Adsorbent for Amoxicillin Removal from Wastewater. J. Clean. Prod. 2021, 284, 124732, doi:10.1016/j.jclepro.2020.124732.
139. Yang, C.; Wang, L.; Yu, Y.; Wu, P.; Wang, F.; Liu, S.; Luo, X. Highly Efficient Removal of Amoxicillin from Water by Mg-Al Layered Double Hydroxide/Cellulose Nanocomposite Beads Synthesized through in-Situ Coprecipitation Method. Int. J. Biol. Macromol. 2020, 149, 93–100, doi:10.1016/j.ijbiomac.2020.01.096.
140. Sayen, S.; Ortenbach-López, M.; Guillon, E. Sorptive Removal of Enrofloxacin Antibiotic from Aqueous Solution Using a Ligno-Cellulosic Substrate from Wheat Bran. J. Environ. Chem. Eng. 2018, 6, 5820–5829, doi:10.1016/j.jece.2018.08.012.
141. Ragauskas, A.J.; Beckham, G.T.; Biddy, M.J.; Chandra, R.; Chen, F.; Davis, M.F.; Davison, B.H.; Dixon, R.A.; Gilna, P.; Keller, M.; et al. Lignin Valorization: Improving Lignin Processing in the Biorefinery. Science 2014, 344, doi:10.1126/science.1246843.
142. Rico-García, D.; Ruiz-Rubio, L.; Pérez-Alvarez, L.; Hernández-Olmos, S.L.; Guerrero-Ramírez, G.L.; Vilas-Vilela, J.L. Lignin-Based Hydrogels: Synthesis and Applications. Polymers (Basel) 2020, 12, 81, doi:10.3390/polym12010081.
143. Li, F.; Wang, X.; Yuan, T.; Sun, R. A Lignosulfonate-Modified Graphene Hydrogel with Ultrahigh Adsorption Capacity for Pb(Ii) Removal. J. Mater. Chem. A Mater. Energy Sustain. 2016, 4, 11888–11896, doi:10.1039/c6ta03779h.
144. Jiang, P.; Li, Q.; Gao, C.; Lu, J.; Cheng, Y.; Zhai, S.; An, Q.; Wang, H. Fractionation of Alkali Lignin by Organic Solvents for Biodegradable Microsphere through Self-Assembly. Bioresour. Technol. 2019, 289, 121640, doi:10.1016/j.biortech.2019.121640.
145. Grishechko, L.I.; Amaral-Labat, G.; Szczurek, A.; Fierro, V.; Kuznetsov, B.N.; Pizzi, A.; Celzard, A. New Tannin–Lignin Aerogels. Ind. Crops Prod. 2013, 41, 347–355, doi:10.1016/j.indcrop.2012.04.052.
146. Domínguez-Robles, J.; Peresin, M.S.; Tamminen, T.; Rodríguez, A.; Larrañeta, E.; Jääskeläinen, A.-S. Lignin-Based Hydrogels with "Super-Swelling" Capacities for Dye Removal. Int. J. Biol. Macromol. 2018, 115, 1249–1259, doi:10.1016/j.ijbiomac.2018.04.044.
147. Agustin, M.B.; Mikkonen, K.S.; Kemell, M.; Lahtinen, P.; Lehtonen, M. Systematic Investigation of the Adsorption Potential of Lignin- and Cellulose-Based Nanomaterials towards Pharmaceuticals. Environ. Sci. Nano 2022, 9, 2006–2019, doi:10.1039/d2en00186a.
148. Gao, B.; Li, P.; Yang, R.; Li, A.; Yang, H. Investigation of Multiple Adsorption Mechanisms for Efficient Removal of Ofloxacin from Water Using Lignin-Based Adsorbents. Sci. Rep. 2019, 9, doi:10.1038/s41598-018-37206-1.
149. Gong, L.; Wu, H.; Shan, X.; Li, Z. Facile Fabrication of Phosphorylated Alkali Lignin Microparticles for Efficient Adsorption of Antibiotics and Heavy Metal Ions in Water. J. Environ. Chem. Eng. 2021, 9, 106574, doi:10.1016/j.jece.2021.106574.
150. Gao, B.; Chang, Q.; Cai, J.; Xi, Z.; Li, A.; Yang, H. Removal of Fluoroquinolone Antibiotics Using Actinia-Shaped Lignin-Based Adsorbents: Role of the Length and Distribution of Branched-Chains. J. Hazard. Mater. 2021, 403, 123603, doi:10.1016/j.jhazmat.2020.123603.
151. Chen, Y.; Liu, J.; Zeng, Q.; Liang, Z.; Ye, X.; Lv, Y.; Liu, M. Preparation of Eucommia Ulmoides Lignin-Based High-Performance Biochar Containing Sulfonic Group: Synergistic Pyrolysis Mechanism and Tetracycline Hydrochloride Adsorption. Bioresour. Technol. 2021, 329, 124856, doi:10.1016/j.biortech.2021.124856.
152. Xiang, W.; Zhang, X.; Luo, J.; Li, Y.; Guo, T.; Gao, B. Performance of Lignin Impregnated Biochar on Tetracycline Hydrochloride Adsorption: Governing Factors and Mechanisms. Environ. Res. 2022, 215, 114339, doi:10.1016/j.envres.2022.114339.